

Impacts of climate change on groundwater resources: a case study of the Sardon catchment, Spain

COLLEN MUTASA
February, 2011

SUPERVISORS:
Dr. Ir. M.W. Lubczynski
Dr. Ir. C. van der Tol



Impacts of climate change on groundwater resources: a case study of the Sardon catchment, Spain

COLLEN MUTASA

Enschede, The Netherlands, February, 2011

Thesis submitted to the Faculty of Geo-Information Science and Earth Observation of the University of Twente in partial fulfilment of the requirements for the degree of Master of Science in Geo-information Science and Earth Observation.

Specialization: Water Resources and Environmental Management

SUPERVISORS:

Dr. Ir. M.W. Lubczynski

Dr. Ir. C. van der Tol

THESIS ASSESSMENT BOARD:

Professor Dr. Z. Su (Chair)

Professor Dr. Okke Batelaan (External Examiner, Vrije Universiteit Brussel)

Errata for MSc Thesis

Collen Mutasa 21525. WREM

24 February 2011

This document lists errors found in the submitted version of Collen Mutasa's MSc thesis: Impacts of climate change on groundwater resources: a case study of the Sardon catchment, Spain together with the corrections.

Location	Original Text	Correction
Abstract lines 23-24	Annual precipitation is expected to decrease by about 5.7%, 5.5% and 125 for the 2020s, 2050s and 2080s respectively.	Annual precipitation is expected to decrease by about 5.7%, 5.5% and 12% for the 2020s, 2050s and 2080s respectively under the A2 scenario.
Page 17, second paragraph line 1 Page 58, last paragraph, line 3	A1B	A1
Page 35, last paragraph, line 4	Figure 5-1	Table 5-1
Page 38, first paragraph, line 7	Figure 4-3	Figure 5-2
Page 48, paragraph 4, line1	Figure 6-2	Figure 6-5
Page 52 under caption Figure 6-7	See Fig 4-3	See Fig 5-2
Page 53, paragraph 1, line 1	Figure 6-9	Figure 6-8
Page 54, paragraph 1, line 2	Figure 6-10	Figure 6-9

DISCLAIMER

This document describes work undertaken as part of a programme of study at the Faculty of Geo-Information Science and Earth Observation of the University of Twente. All views and opinions expressed therein remain the sole responsibility of the author, and do not necessarily represent those of the Faculty.

ABSTRACT

Groundwater forms the main source of water for drinking and irrigation particularly in water limited environments where surface water resources are unreliable and potential evapotranspiration (PET) is large compared to rainfall. Its sustainability however is threatened by climate change. The impacts of climate change on groundwater resources of semi arid Sardon area in Spain characterized by negligible human impact are investigated. First, historical climate data of the catchment is analysed to determine whether there has been any climate change in the catchment. A statistical downscaling model, the Statistical Downscaling Model (SDSM) is used to downscale present and future daily precipitation and temperature data from the UK Hadley Centre General Circulation Model (GCM), HadCM3. Two future emission scenarios, A2 (medium-high) and B2 (medium-low) are considered for three 30 year periods from 2010 to 2039(2020s), 2040 to 2069(2050s) and 2070 to 2099(2080s). Downscaling was done to obtain finer resolution output from the coarse resolution of GCM, so that it matched with the Sardon catchment scale. This output provided input rain and PET for the lumped parameter hydrological model, pyEARTH 1-D which simulated recharge and actual evapotranspiration (ET_a) for the 2020s. The recharge from pyEARTH was further applied as uniform input over the entire Sardon catchment in the MODFLOW model calibration. A calibrated groundwater flow model MODFLOW was finally run in transient prediction over 60 stress periods to determine the impacts of climate change on groundwater resources for the 2020s for both the A2 and B2 scenarios. Results from trend analysis of maximum and average temperatures reveal evidence of climate change in the catchment. No significant trends were noted for minimum temperatures and precipitation. The downscaled future climate also showed that mean daily minimum temperatures, maximum temperatures and average temperatures are forecast to increase by up to 5.0°C, 7.0° C and 5.9°C respectively by the end of the XXI century when compared to the baseline period of 1961 to 1990. More warming is expected in summer than in winter and higher temperatures are projected for the A2 than B2 scenario. Annual precipitation is expected to decrease by about 5.7%, 5.5% and 125 for the 2020s, 2050s and 2080s respectively. For the B2 scenario, annual precipitation decreases by 4.9%, 7.2% and 3.4% for the 2020s, 2050s and 2080s respectively when compared to the baseline. Recharge will decrease by 26.9% for the A2 scenario and 21% for the B2 scenario when compared to the baseline for the 2020s. In response to the decreased recharge and precipitation, groundwater storage will decrease by 24.2% and 10.9% under the A2 and B2 scenarios respectively for the 2020s period. The total amount of water lost as drain will be greater under the A2 scenario than B2 scenario and recharge will be higher under the B2 scenario than the A2 scenario.

ACKNOWLEDGEMENTS

First and foremost I wish to thank the Netherlands government for providing me with a scholarship through the Netherlands Fellowship Programme (NFP) that enabled me to pursue my studies.

I am also greatly indebted to my supervisors, Dr M. W. Lubczynski and Dr. C. Van der Tol for their critical comments, suggestions and guidance throughout the thesis period. I also wish to express my sincere gratitude to staff who helped me in one way or another during this thesis phase especially, Mr. G. N. Parodi for his guidance during fieldwork and Drs. J. B. Boudewijn de Smeth for his assistance during laboratory analyses.

Special thanks also go to my student advisor Tanvir Hassan for useful suggestions throughout the thesis writing and assistance with laboratory work, Alain Frances for his guidance and patience, Dr. L. Unganai, Dr. A. Murwira and Dr. M. Shongwe for useful suggestions during informal chats.

I am very grateful to Dr. C. Dawson, Dr. R. L. Wilby and Girma Yimer Ebrahim for their help in using the Statistical Downscaling Model.

Lastly I wish to express my appreciation of useful discussions we held with WREM 2009-2011 class colleagues.

TABLE OF CONTENTS

Abstract.....	i
Acknowledgements.....	ii
List of figures.....	v
List of tables.....	vi
ABBREVIATIONS and ACRONYMS.....	vii
1. INTRODUCTION.....	1
1.1. Background.....	1
1.2. Research Problem.....	1
1.3. Research Questions.....	2
1.4. Research Objectives.....	2
1.4.1. General Objective.....	2
1.4.2. Specific Objectives.....	2
1.5. Literature Review.....	2
1.6. Hypothesis.....	3
1.7. Assumptions.....	3
1.8. Thesis Outline.....	3
2. STUDY AREA.....	4
2.1. Location.....	4
2.2. Hydrological monitoring.....	4
2.3. Environmental conditions.....	5
2.3.1. Meteorological conditions.....	5
2.3.2. Land cover and land use.....	7
2.3.3. Hydrological conditions.....	8
2.3.4. Hydrogeological conditions.....	8
3. DATA COLLECTION AND ANALYSIS.....	11
3.1. Double ring infiltrometer tests.....	11
3.2. Augering.....	12
3.3. Groundwater Level Measurements.....	13
4. THEORETICAL BACKGROUND.....	16
4.1. Climate Modeling.....	16
4.1.1. General Circulation Models.....	16
4.1.2. Hadley Centre Coupled Model, version 3 (HadCM3).....	16
4.1.3. Emission scenarios.....	16
4.1.4. Baseline Climate.....	17
4.1.5. Downscaling GCM output.....	18
4.1.6. Statistical Downscaling Model (SDSM).....	21

4.2.	Hargreaves Equation.....	24
4.3.	Groundwater recharge modeling with py EARTH 1-D MODEL.....	25
4.3.1.	Methods of estimating recharge.....	25
4.3.2.	EARTH MODEL.....	26
4.4.	Groundwater modeling.....	31
4.4.1.	Conceptual model.....	31
4.4.2.	Numerical Model.....	31
5.	METHODOLOGY.....	33
5.1.	Generating climate time series.....	33
5.2.	Trend Analysis.....	34
5.3.	Statistical Downscaling.....	35
5.4.	Converting climate model output into groundwater recharge.....	37
5.5.	Groundwater Modeling.....	37
5.5.1.	Model Set up and boundaries.....	37
5.5.2.	Model Calibration.....	38
5.5.3.	Time Discretization.....	40
5.5.4.	Water balance.....	40
6.	RESULTS AND DISCUSSION.....	41
6.1.	Generating climate time series.....	41
6.2.	Trend Analysis.....	42
6.3.	Downscaling GCM Output.....	42
6.4.	Recharge Modeling with pyEARTH.....	48
6.5.	Groundwater Modeling.....	49
7.	CONCLUSION AND RECOMMENDATIONS.....	57
7.1.	Conclusion.....	57
7.2.	Recommendations.....	57
	List of references.....	59
8.	Appendices.....	62

LIST OF FIGURES

Figure 2-1: Location of the Sardon catchment	4
Figure 2-2: Mean monthly rainfall (2000-2007) for Trabadillo station.....	5
Figure 2-3 : Mean monthly minimum, maximum and average temperature for Trabadillo station.....	6
Figure 2-4: Daily PET for Trabadillo station, September 2004 –September 2008	7
Figure 2-5: Mean monthly PET for Trabadillo station.....	7
Figure 2-6: Schematic cross section of the study area (Lubczynski and Gurwin, 2005)	9
Figure 3-1: Spatial distribution of double ring experiment sites.....	11
Figure 3-2: Spatial distribution of augering sites.....	12
Figure 3-3: The monitoring network of piezometers in the Sardon Catchment	15
Figure 4-1: A schematic illustrating the general approach to downscaling. (Adapted from Wilby and Dawson 2007).....	21
Figure 4-2: EARTH-1D Model flowchart. Source :(Lee & Gehrels, 1990)	30
Figure 5-1: Spatial distribution of AEMET stations relative to Trabadillo	34
Figure 5-2: Model layer 2 and the 5 calibration piezometers.....	39
Figure 6-1: Time series of precipitation and temperature for Trabadillo station	41
Figure 6-2: Validation results of SDSM downscaling at Trabadillo station.....	43
Figure 6-3: Observed 1961-90 mean daily precipitation, min and max temperature and simulated data....	45
Figure 6-4: Comparison of current (1961-1990) mean daily precipitation, average temperature, minimum and maximum temperatures with future HadCM3 simulated data for the A2 and B2 scenarios.....	47
Figure 6-5: Calibration graphs for the period 2004 to 2008	48
Figure 6-6: Calibration values of K, Sy and Ss for the two model layers.....	50
Figure 6-7: MODFLOW calibration head data in piezometers: Pgb0, Pgi0, Pmu1, Psd1 and Ptb2 (see Fig4-3) for the calibration period 2004-2008	52
Figure 6-8: Prediction of groundwater levels of the 5 piezometers for the A2 and B2 scenarios (2010-2039)	53
Figure 6-9: Graphical Representation of water balance components for the A2 and B2 scenarios for 2010-2039	54
Figure 6-10: Variation of recharge, drain and storage for the A2 and B2 scenario for 2010-39.....	56

LIST OF TABLES

Table 3-1: Soil hydraulic parameters for the Sardon catchment	13
Table 4-1: The Emission Scenarios of the IPCC Special Report on Emission Scenarios (SRES)	17
Table 4-2: Comparative summary of the relative merits of statistical and dynamical downscaling techniques (adapted from Wilby and Wigley, 1997).....	20
Table 4-3: Large-scale atmospheric variables from the NCEP reanalysis and HadCM3 simulation	23
Table 4-4: Parameter configuration for the EARTH Model.....	31
Table 5-1: Large scale predictor variables selected for SDSM downscaling.....	36
Table 6-1: Trend testing results.....	42
Table 6-3: Model calibration results.....	43
Table 6-2: Results of pyEARTH 1-D Modeling.....	49
Table 6-4: Change in groundwater levels for the 5 piezometers for the 2020s.....	53
Table 6-6: Water balance components under the A2 and B2 scenarios for 2010-2039.....	54

ABBREVIATIONS AND ACRONYMS

A2a	Medium-high Emissions Scenario
ADAS	Automatic data acquisition system
AEMET	Agencia Estatal de Meteorología
AOGCM	Atmosphere-Ocean General Circulation Model
B2a	Medium-low Emission scenario
CGCM1	Canadian Global Climate Model1
DEM	Digital Elevation Model
EARTH	Extended model for Aquifer Recharge and soil moisture Transport through the unsaturated Hard rock
ETa	Actual Evapotranspiration
GCM	General Circulation Model/Global Climate Model
HadCM3	Hadley Centre Coupled Model version3
IPCC	Intergovernmental Panel on Climate Change
IPCC TAR	Intergovernmental Panel on Climate Change Third Assessment Report
IRBM	Royal Institute of Meteorology of Belgium
Ks	Saturated hydraulic conductivity
LARS-WG	Long Ashton Research Station Weather Generator
LAM	Limited Area Model
LINRES	Linear Reservoir Routing
m.a.s.l	Metres above sea level
MAXIL	Maximum Interception Loss
m.b.g.s	Metres below ground surface
MODFLOW	Modular Three-Dimensional Finite-Difference Groundwater Flow Model
NCEP	National Centre for Environmental Prediction
PET	Potential Evapotranspiration
RCM	Regional Climate Model
SATFLOW	Saturated Flow
SDSM	Statistical Downscaling Model
SOMOS	Soil Moisture Storage
SRES	Special Report on Emission Scenarios
UNFCCC	United Nations Framework Convention on Climate Change
WMO	World Meteorological Organization

1. INTRODUCTION

1.1. Background

Climate change is one of the biggest challenges facing mankind today. Several definitions of climate change have been put forward by a number of scientific bodies. One such definition by the United Nations Framework Convention on Climate Change (UNFCCC, 1992) refers to climate change as, “a change of climate which is attributed directly or indirectly to human activity that alters the composition of the global atmosphere and which is in addition to natural climate variability observed over comparable time periods.”

There is growing evidence that global climate is changing. According to the Intergovernmental Panel on Climate Change (IPCC, 2001a), global mean temperatures have risen 0.3 – 0.6°C since the late 19th century and global sea levels have risen between 10 and 25cm. (McCarthy *et al.*, 2001) note that global temperatures will continue to rise by between 1.4 and 5.8°C by 2100 relative to 1990 due to the emissions of greenhouse gases. As the warming process continues, it will bring about numerous environmental problems, among which the most severe will relate to water resources; (Loaiciga *et al.*, 1996; Milly *et al.*, 2005; Holman, 2006; IPCC, 2007). Temperature increases also affect the hydrologic cycle by directly increasing evaporation of available surface water and vegetation transpiration. Consequently these changes can influence precipitation amounts, timings and intensity rates and indirectly impact the flux and storage of water in surface and subsurface reservoirs (i.e. lakes, soil moisture, groundwater) (Toews, 2003).

Groundwater is the main source of water for drinking and irrigation in low rainfall arid and semi arid areas where there are no significant surface water sources. This is because groundwater is slow to respond to changes in precipitation regimes and thus acts as a more resilient buffer during dry spells. In fact worldwide, more than 2 billion people depend on groundwater for their daily supply (Kemper, 2004). Furthermore groundwater forms the largest proportion (~ 97%) of the world’s freshwater supply. By maintaining surface water systems through flows into lakes and base flow to rivers, groundwater performs the crucial role of maintaining the biodiversity and habitats of sensitive ecosystems (Tharme, 2003). The role of groundwater is becoming even more prominent as the more accessible surface water resources become less reliable and increasingly exploited to support increasing populations and development (Bovolo *et al.*, 2009).

The effects of global warming on water resources, and especially on groundwater, will depend on the groundwater system, its geographical location and changes in hydrological variables (Alley, 2001; Huntington, 2006; Sophocleous, 2004) . Knowing how climate change will affect groundwater resources is thus important as it will allow water resources managers to make more rational decisions on water allocation and management (Sullivan, 2001) and enable the formulation of mitigation and adaptation measures.

1.2. Research Problem

Despite groundwater’s significance, there has been comparatively little research conducted on groundwater relative to surface water resources, particularly in the context of climate change impact

assessment (Bates *et al.*, 2008). Most of the climate change impact studies have concentrated on surface water resources (Mimikou *et al.*, 2000; Chistensen *et al.*, 2004; Graham, 2004; Payne *et al.*, 2004; Van Rheenen *et al.*, 2004; Krysanova *et al.*, 2005; Drogue *et al.*, 2004; Gellens, 1991; Menzel and Burger, 2002; Pfister *et al.*, 2004).

Furthermore no climate change impact studies on groundwater resources have been conducted in the proposed study area, Sardon, a small catchment of area, 80 km². Most of the research conducted in this catchment has focused on groundwater modelling, tree transpiration, groundwater recharge modelling and the characterisation of the subsurface e.g. (Attanayake, 1999; Berhe, 2010; Cornejo, 2000; Lubczynski & Gurwin, 2005; Ontiveros, 2009; Rajapakse, 2009; Shakya, 2001; Tesfai, 2000).

1.3. Research Questions

- Is there any climate change in the Sardon catchment and if so what is its impact on recharge and groundwater resources?
- How to integrate meteorological data of different locations and time in the study area?
- What is the most suitable General Circulation Model (GCM) and/or downscaling model to simulate climate change in the study area?
- How can climate model outputs be used to predict groundwater recharge?

1.4. Research Objectives

1.4.1. General Objective

- To quantify the impacts of climate change on groundwater resources of a semi-arid area such as the Sardon Catchment in Spain.

1.4.2. Specific Objectives

- To generate a daily record of precipitation and temperature (and PET) for Trabadillo, representative of the Sardon Study area based on the longest available rainfall and temperature data of neighbouring stations.
- To downscale climate change scenario output from a GCM, the HadCM3 for the Sardon catchment using a Statistical Downscaling Model (SDSM).
- To estimate past and future recharge in the study area using the pyEARTH 1-D Model
- To use a calibrated MODFLOW model to simulate future scenarios in groundwater resources in the study area.
- To evaluate the impacts of climate change on groundwater resources.

1.5. Literature Review

A number of researchers have studied the effects of climate change on groundwater resources. Different hydrologic and groundwater flow models were used in the studies.

In a study of the Grand River watershed in Ontario, Canada, (Jyrkama & Sykes, 2007) used HELP3 to simulate past and future recharge. They used temperature and precipitation climate change scenarios based on the predictions of IPCC (2001). Results showed that an increase in rainfall as a result of climate change led to an increase in recharge. The increase though, varied from place to place due to differences in land use and soil types.

Brouyere *et al.*, 2004 studied the impacts of climate change in a small aquifer, the Geer Basin in Belgium. They used an integrated hydrological model (MOHISE) which is composed of three interacting sub models: a soil model, a surface water model and a groundwater model which are dynamically linked. Climate change scenarios were prepared by the Royal Institute of Meteorology of Belgium (IRBM) based on experiments done with seven GCMs. They found that future climate changes could result in a decrease in groundwater levels. However no seasonal changes were noted. In another independent study in the same basin (Goderniaux *et al.*, 2009) combined a coupled surface-subsurface flow model, HydroGeosphere with climate change scenarios from six regional climate models assuming the Special Report on Emission Scenarios(SRES) A2(medium-high) emission scenario. Results showed a significant decrease of up to 8m in groundwater levels by 2080.

In (Scibek & Allen, 2006a), the responses of two small aquifers to climate change, one in western Canada and the other in the United States, were compared. One aquifer is recharge dominated while the other is connected to a river. Downscaled climate change scenarios from the Canadian Global Climate Model1 (CGCM1) GCM were used in combination with a groundwater flow model, MODFLOW. Small changes in groundwater levels forced by changes in recharge were noted. The results show that the climate region, distribution of material properties, nature of surface water - groundwater interaction and aquifer geometry influence the impact on water levels.

In yet another study in the United States, Crowley & Lukkonen (2003) investigated the impact of climate change on groundwater levels in the Lansing area in Michigan. They considered the 20 years centred around 2030 as the future changed climate condition and the baseline as the period 1961 to 1990. Groundwater recharge was estimated from streamflow simulations and from variables derived from GCMs. Their results indicated that groundwater levels would increase or decrease depending on the GCM used to simulate the future.

1.6. Hypothesis

- Groundwater resources in the Sardon catchment will be influenced by climate change.

1.7. Assumptions

- Human activities such as agriculture and land use changes have negligible direct effect on groundwater resources in the study area.
- Groundwater abstraction is negligible in the study area.

1.8. Thesis Outline

Chapter 1 gives a general introduction comprising of background, problem statement, research objectives, research questions, literature review, hypotheses and assumptions. Chapter 2 looks at Data collection and analysis. Chapter 3 gives a description of the study area while Chapter 4 is about the Theoretical Background of the study. Chapter 5 provides information on the methodology while chapter 6 is about Results and Discussion. Chapter 7 provides the Conclusion and Recommendations. This is followed by a list of references and appendices.

2. STUDY AREA

2.1. Location

The Sardon catchment is located in Salamanca province in central western Spain, some 50 km west of Salamanca city. The catchment is part of the Rio Tormes river basin and lies between latitudes 41° 01'-41° 08'N and 6° 07'-6°13'W longitudes and covers an area of approximately 80km² characterized by low human population. The elevation varies from about 740 m a.s.l at the Sardon river outlet point to about 840 m a.s.l at the highest southern boundary with fairly undulating topography. The area is comprised of impermeable schists and massive granite at the southern boundary, massive granites at the western and northern boundaries and fractures filled with quartzite material at the eastern boundary (Lubczynski & Gurwin, 2005). Geomorphologically, the area shows two distinct units, gently undulating western part and a steeper undulating eastern part, the two divided by the Sardon regional fault (Attanayake, 1999).

2.2. Hydrological monitoring

The Sardon catchment is equipped with an automated monitoring network which includes a meteorological Automatic Data Acquisition System (ADAS) station and automated monitoring loggers for measuring hydraulic head variation and soil moisture. There are two automatic data stations (ADAS), situated in Trabadillo and Muellesdes and these are capable of recording rainfall, wind speed, temperature, relative humidity and solar radiation data on an hourly basis.

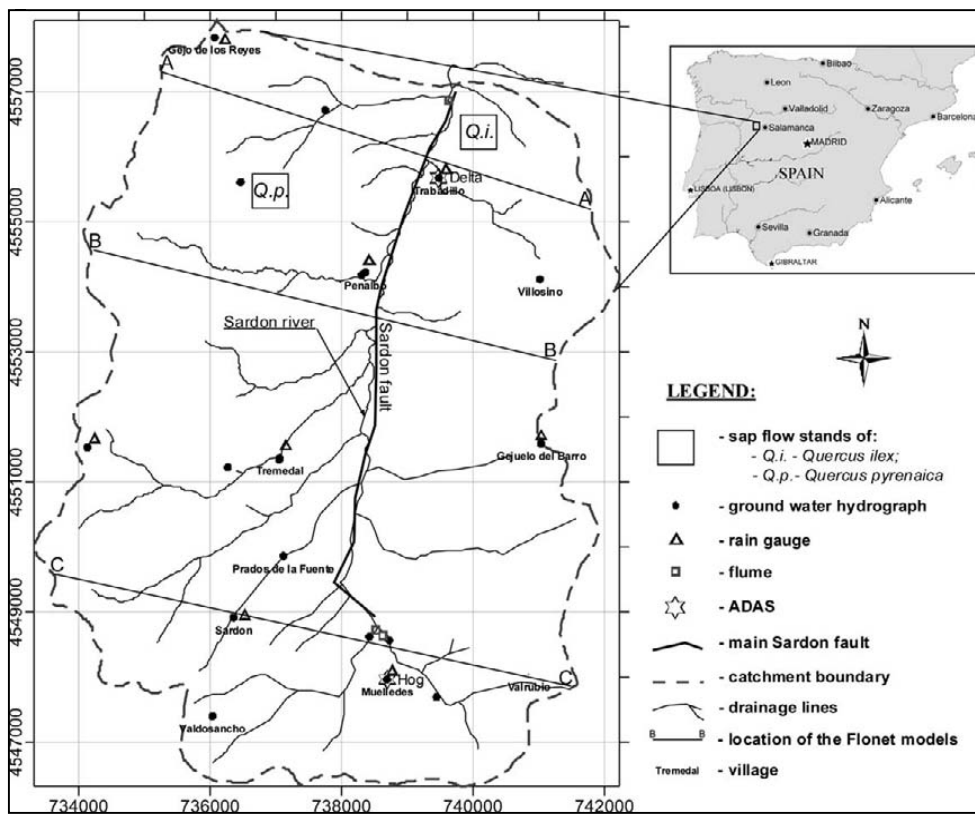


Figure 2-1: Location of the Sardon catchment

2.3. Environmental conditions

Sardon is a semi-arid area with an annual precipitation of about 500mm. The warmest and driest months are July and August with an average temperature of 22°C, a potential evapotranspiration (PET) of 5mm per day and rainfall averaging less than 20 mm per month. The coldest months are January and February with an average temperature of 5°C, while the wettest months are November and December with rainfall above 100 mm per month and the lowest PET of 0.5 mm per day (Lubczynski & Gurwin, 2005).

2.3.1. Meteorological conditions

Hourly precipitation and temperature data for Trabadillo and Muelledes date back to 1997 and 1998 respectively. However there are a lot of gaps of missing data ranging from a few days to years for both stations. The longest continuous record for Trabadillo is from about September 2003 to April 2008. Figures 3-2 to 3-5 show graphs of mean monthly rainfall and temperature for Trabadillo for the periods 2000-2007 and 2004-2006 respectively.

Rainfall

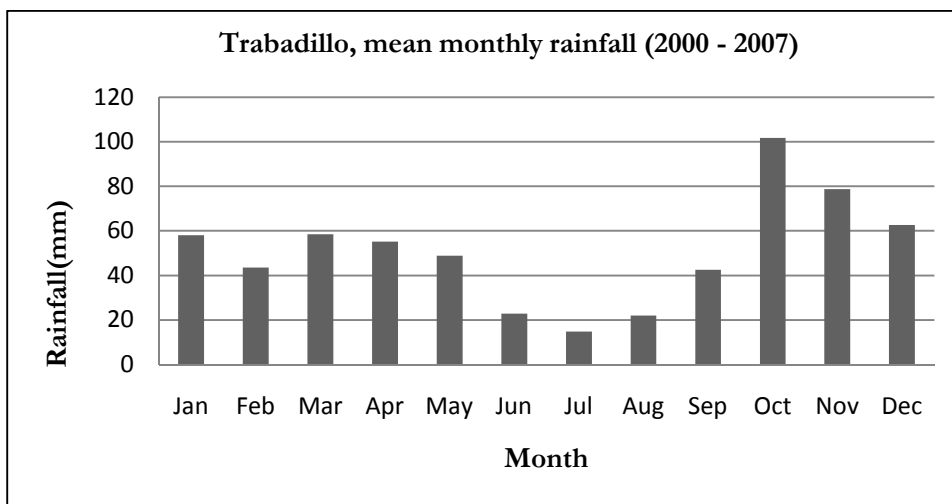


Figure 2-2: Mean monthly rainfall (2000-2007) for Trabadillo station

Temperature

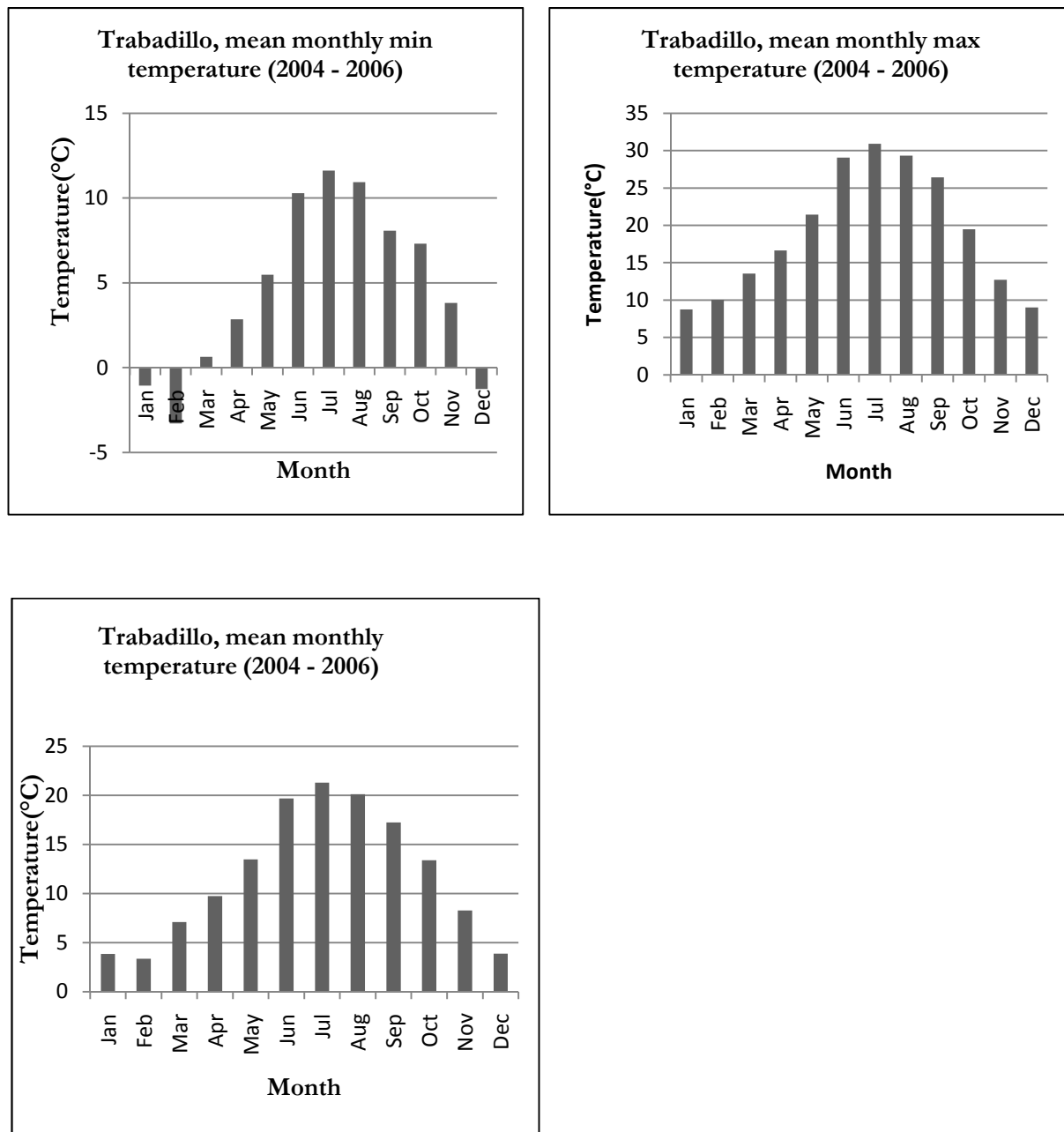


Figure 2-3 : Mean monthly minimum, maximum and average temperature for Trabadillo station

Evapotranspiration

Evapotranspiration dominates the water budget in arid and semi-arid areas where potential evapotranspiration is much greater than the annual rainfall. Evapotranspiration can be defined as the process by which water is returned to the atmosphere by a combination of evaporation and transpiration (Andreasson *et al.*, 2009). It is therefore a combination of evaporation from open water bodies, evaporation from soil surfaces and transpiration from soil by plants. Evapotranspiration can be estimated from meteorological data and is dependent on factors such as wind speed, humidity, temperature and radiation. It generally increases with increasing precipitation. Evapotranspiration can be divided into two classes, potential evapotranspiration (PET) and actual evapotranspiration (ETa).

Actual evapotranspiration

This is the amount of water that actually returns to the atmosphere depending on the availability of water. It can be estimated by noting fluctuations of groundwater table (Freeze & Cherry, 1979) as well as modelling approaches such as the pyEARTH 1-D model.

Potential Evapotranspiration

This describes water loss that will occur under given climate conditions with no deficiency of water in the soil for the use by vegetation (Thornthwaite, 1948). It is highest during dry summer periods and lowest during rainy winter periods.

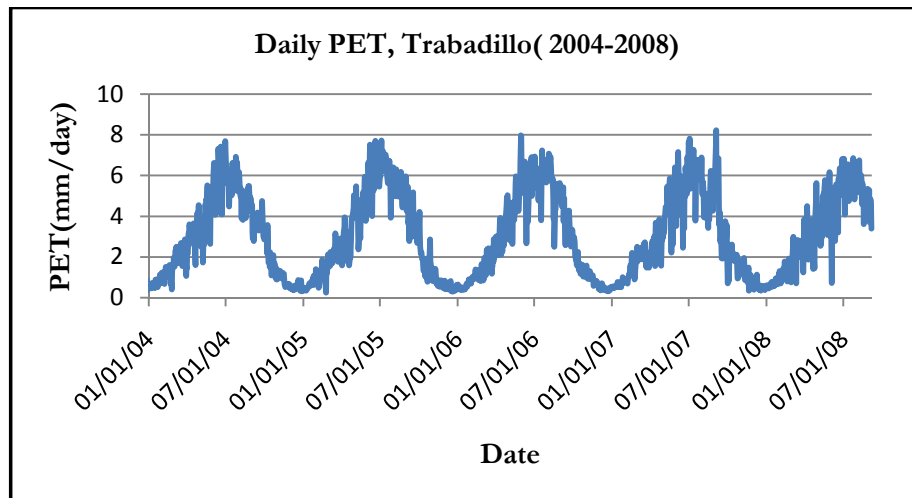


Figure 2-4: Daily PET for Trabadillo station, September 2004 –September 2008

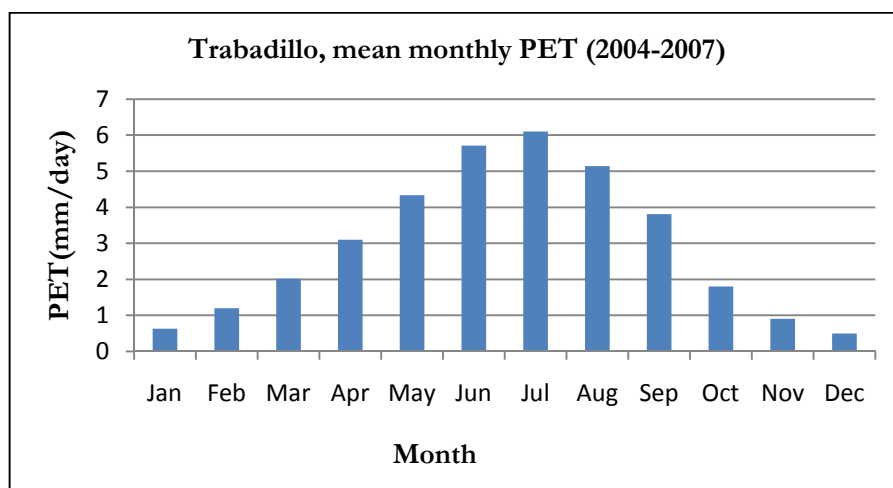


Figure 2-5: Mean monthly PET for Trabadillo station

2.3.2. Land cover and land use

The *Quercus* (oak) tree genus is the dominant tree in the study area and two types of species can be identified: evergreen oak *Quercus ilex* and the broad-leaved deciduous oak *Quercus pyrenaica* locally named 'encina' and 'roble' respectively. The evergreen *Quercus ilex* (*Q. ilex*) typically grows to heights of about 20-27m with a trunk of approximately 1m in diameter although in the study area tree heights are about 6m. It is considered water use efficient due to its small leaves which minimise evaporative losses. *Q. ilex* have been observed in times of acute water stress or shortage to be able to lift up groundwater through their roots, release it into the upper soil layer due to a water potential gradient. The water released in upper soil layers is then reabsorbed by shallow roots and transpired. This mechanism is termed hydraulic lift (David *et al.*, 2007). These groundwater uptake abilities allow for the classification of *Q. ilex* in Mediterranean weather as being a phreatophyte. The *Quercus pyrenaica* can grow up to 25m with a trunk of approximately 0.4m in diameter. The *Quercus pyrenaica* grow in clusters. They have a potent rooting system with a deep tap root which develops several horizontal roots, mainly in the shallow subsurface allowing the development of peripheral vegetation around the trunk. However it has not been proved that the *Quercus pyrenaica* can tap water from groundwater (phreatophyte behaviour). The area under the sparsely distributed trees is covered with *Cytisus scoparius* (Scotch Broom) shrub and short grass (Shakya, 2001). The *Cytisus scoparius* typically grows 1-3m tall with main stems up to 5cm thick. However in the Sardon study area *Cytisus scoparius* does not exceed a height of 1m. The natural woody-shrub vegetation is used mainly for pasture because the soils contain large proportions of weathered granite, which make them generally unsuitable for agriculture.

2.3.3. Hydrological conditions

The Sardon River is mostly dry during the period June to October. However, during the wet period the flow occurs as direct runoff in response to high intense rainfall showers due to the thin, highly permeable upper unconsolidated layer with low retention capacity (Shakya, 2001). Also in rainy seasons, during and shortly after heavy rain showers, temporary flooding of the terrain depressions with temporal saturation of vadose zone may also take place (Lubczynski & Gurwin, 2005). The groundwater flow pattern follows the regional Sardon fault zone which then transmits the water towards the northern outlet.

2.3.4. Hydrogeological conditions

The geology and hydrogeology of the catchment is strongly influenced by the prevailing granitic rock composition. The regional flow system is ruled by the interconnected fractures in the region (Shakya, 2001). The Sardon brittle shear zone seems to control the morphology of the catchment (Tesfai, 2000).

In the catchment, three layers can be identified, namely:

- A top unconsolidated layer composed of weathered and alluvial deposits (0-5m). This layer is limited in spatial extent.
- A fractured granite layer with intercalations of granodiorites, schists, gneiss and quartzites which outcrops extensively in the study area. Its depth varies from 60m b.g.s. in the central part of the catchment to a few metres in the upland areas.
- A massive granite layer with some gneiss inclusions which forms the impermeable rock basement (aquiclude) and is deepest in the centre and shallowest at catchment boundaries (Lubczynski & Gurwin, 2005).

The groundwater table, which shows a concentric pattern influenced by the fault zone, is shallow in the river valleys (0-3m b.g.s) and deeper at the watershed divides (2-6m b.g.s.), a typical characteristic in granitic areas.

Groundwater use can be considered negligible for it is only utilized by cattle farms. Farms use this resource by extracting from man made ponds that dry in summer due to seasonal groundwater table lowering and surface evaporation (Lubczynski & Gurwin, 2005).

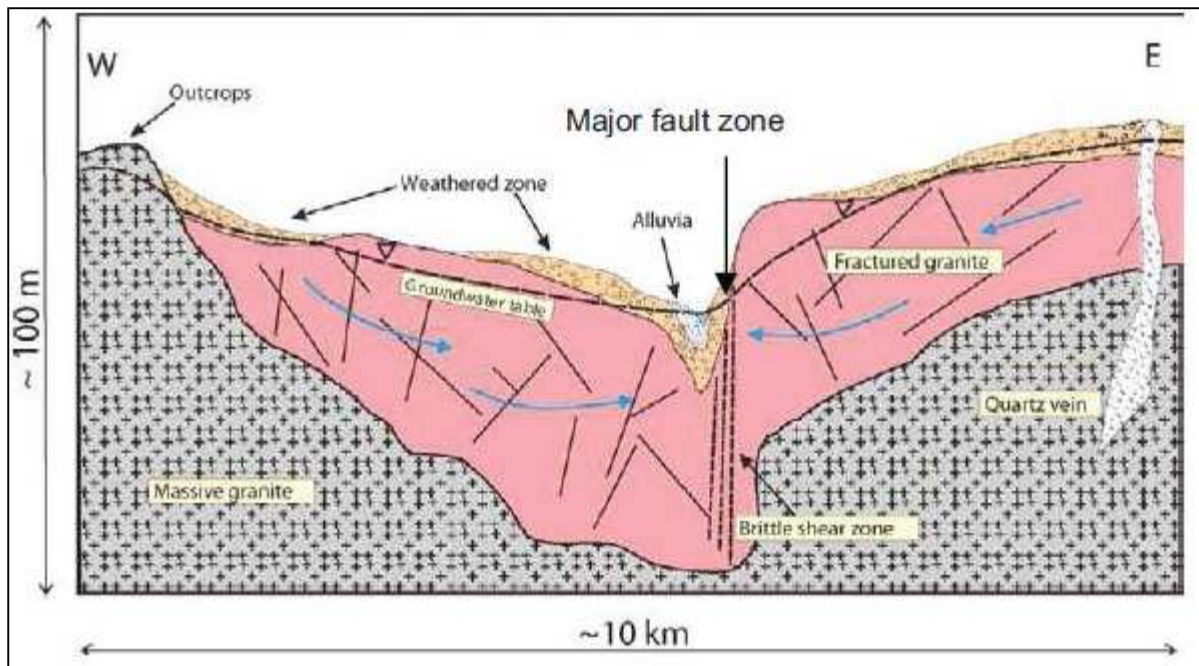


Figure 2-6: Schematic cross section of the study area (Lubczynski and Gurwin, 2005)

3. DATA COLLECTION AND ANALYSIS

Data is required mainly as input into the recharge and groundwater flow models or for calibration purposes. This data includes hydraulic conductivity, soil moisture, root zone depth and storativity. Both primary and secondary data were collected. In the field, hand augering and double ring experiments were conducted. The locations of sampling were randomly selected however with the objective of covering the whole catchment. The data was later processed and interpreted.

3.1. Double ring infiltrometer tests

The double ring infiltrometer is an instrument that is used to determine the rate of infiltration of water into the soil. The rate of infiltration is determined by the amount of water that infiltrates into the soil per surface area, per unit of time. If water is flowing in one-dimension under steady state conditions, and a unit gradient is present in the underlying soil, the infiltration rate is approximately equal to the saturated hydraulic conductivity (Dingman, 2002). It is the rate of this process, relative to the rate of water supply that determines how much soil water will enter the unsaturated soil zone and how much, if any will run off (Hillel, 1982). In its construction, the double ring infiltrometer consists of inner and outer steel rings of different diameters that are driven into the ground and water poured inside. The drop in the water level of the inside ring is then recorded at different time intervals until a constant rate is attained. The infiltration capacity decreases with time until it reaches a constant value which approximates to the saturated hydraulic conductivity. The purpose of the outer ring is to create a one dimensional vertical flow of water from the inner ring and thus prevent lateral flow. At least two tests were done at each site so as to get a mean result of infiltration rate.

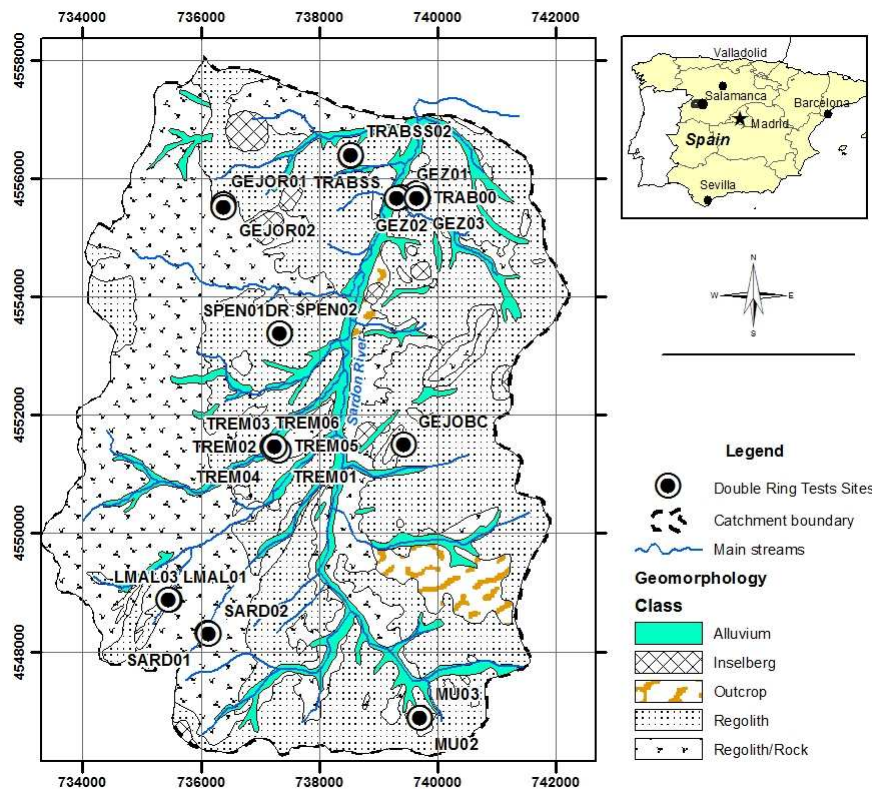


Figure 3-1: Spatial distribution of double ring experiment sites

3.2. Augering

Soil sampling was conducted in the catchment by way of hand augering. The soil samples were collected at different places and depths to determine soil moisture parameters such as hydraulic conductivity and soil moisture at field capacity. The determination of saturated permeability was done using the laboratory permeameter, with the constant head method being used for most of the soil samples. The falling head method was used to analyse soil samples with low permeability. Values of saturated hydraulic conductivity obtained using the double ring infiltrometer were compared with those derived using the permeameter as shown in table 2.1 Permeability refers to the capacity of a soil to drain off water and the permeability coefficient (K-factor) gives a measure of permeability. The WP4-T Dewpoint PotentialMeter instrument was used to derive soil parameters for the plotting of soil water retention curves from which soil moisture at wilting point was derived.

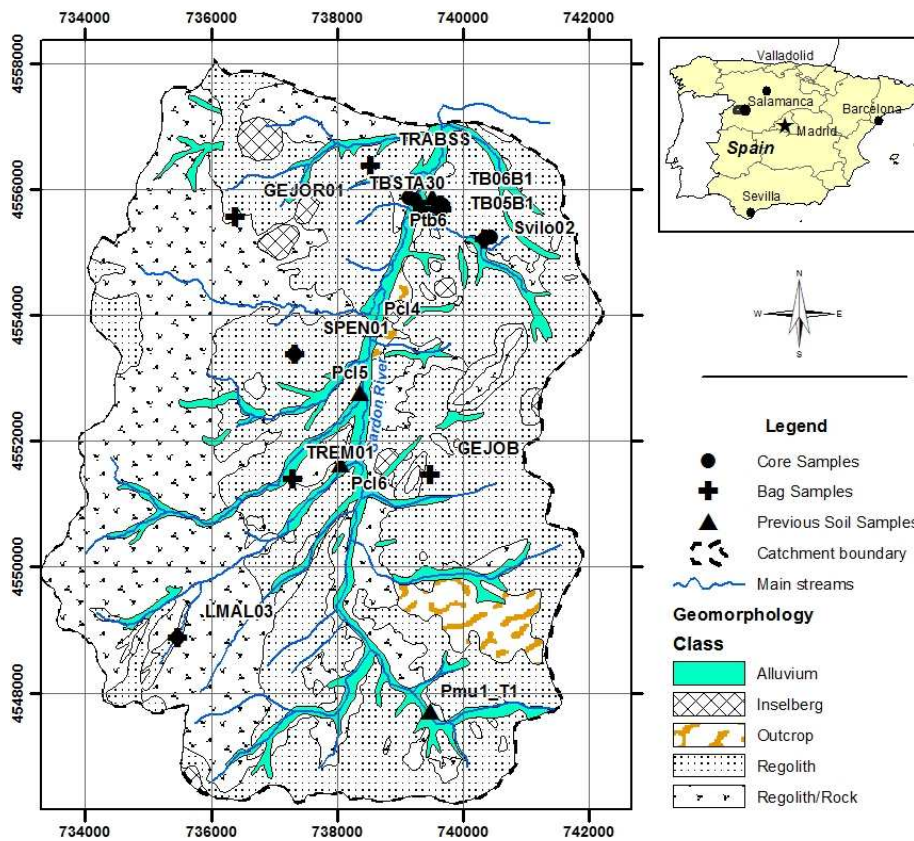


Figure 3-2: Spatial distribution of augering sites

Table 3-1: Soil hydraulic parameters for the Sardon catchment

ID	Place	X [UTM]	Y [UTM]	K _{sat} (mm/day)		θ _{fc}	θ _{wp}	P [g/cm ³]	W [g/g]	θ [cm ³ /cm ³]	Porosity
				Pmeter	DRI						
TB-E-100	Trabadillo	739368	4555676	1340		0.08		1.77	0.13	0.22	0.33
LAMATA	La Mata	739656	4555667	4638	4937	0.08	0.05	1.64	0.17	0.28	0.38
GD2.1	La Mata	739353	4555611	1281	1916	0.07	0.48	1.23	0.36	0.44	0.54
SPEN1-05R	Penalbo	737324	4553383	3771	1495	0.06		1.81	0.15	0.27	0.32
GD1.1	La Mata	739381	4555666	55197	1665	0.12	0.13	1.59	0.18	0.28	0.40
SVIL12-06R	Villosino	740348	4555212	39382		0.10	0.17	1.72	0.16	0.28	0.35
GD3.1	La Mata	739386	4555380	42501	1824	0.08	0.04	1.78	0.13	0.22	0.33
TB-E-75	Trabadillo	739368	4555676	1757	2902	0.09		1.77	0.14	0.25	0.33
TB-E-50	Trabadillo	739368	4555676	4836	1913	0.07		1.83	0.14	0.25	0.31
SPEN1-02R	Penalbo	737324	4553383	542		0.10		1.50	0.23	0.35	0.43
TB-E-25	Trabadillo	739368	4555676	55		0.12		1.87	0.11	0.20	0.29
SVIL02-02R	Villosino	740348	4555212	1317		0.13		1.79	0.16	0.28	0.32
SVIL-01R	Villosino	740452	4555232	53310		0.12	0.11	1.85	0.13	0.24	0.30
LMAL-03	Los Malones	735460	4548868	143	1008	0.14	0.05	1.78	0.15	0.26	0.33
TB08R	Trabadillo	739140	4555870	126		0.14	0.04	1.78	0.15	0.26	0.33
GD1.2	La Mata	739381	4555666	1281		0.16	0.05	1.85	0.12	0.23	0.30
TB-08R2	Trabadillo	739140	4555870	23		0.11		1.90	0.14	0.27	0.28
LMAL-04	Los Malones	735460	4548868	67	2029	0.16		1.75	0.14	0.25	0.34
SDRILL-02R	Trabadillo	736104	4548287	601		0.11	0.05	1.52	0.23	0.35	0.43
TREMss01	Tremedal	737289	4551394		3703		0.02				
GEJOB01	Gejo del Barro	739479	4551461		3443		0.05				
MU02	Mulledes	739697	4546864		3600						
GEJOR	Gejo del los Reyes	736383	4555557		4361						

K_{sat}: saturated hydraulic conductivity; P_{meter}: permeameter; DRI: Double ring infiltrometer; θ_{fc}: soil moisture at field capacity; θ_{wp}: soil moisture at wilting point; ρ: bulk density; w: gravitational soil moisture content; θ: volumetric soil moisture content

3.3. Groundwater Level Measurements

Groundwater level measurements were taken using two methods, namely automated monitoring loggers and manually using a sounding device attached to a measuring tape.

a) Loggers

The automated monitoring loggers installed at some piezometers measure the hydraulic head on an hourly basis. Data is available from 2003 to 2008 in six locations in the catchment. Absolute loggers measure the absolute pressure above the top of an immersed logger. When the logger is placed below the water table in the well or piezometer, it records the pressure of the column of water above it. A separate logger measures atmospheric pressure. As the groundwater table rises or falls, the absolute pressure will rise or fall also.

The pressure head exerted by the column of water above the logger is obtained from the relationship:

Pressure Head = Absolute Pressure - Atmospheric Pressure

b) Sounding Device

The sounding device consists of a measuring tape attached to a probe equipped with an acoustic and light signal. The probe is lowered into a piezometer or well and when it gets in contact with the water, a beep sound is produced and a light goes on. The water level is then read from the measuring tape.

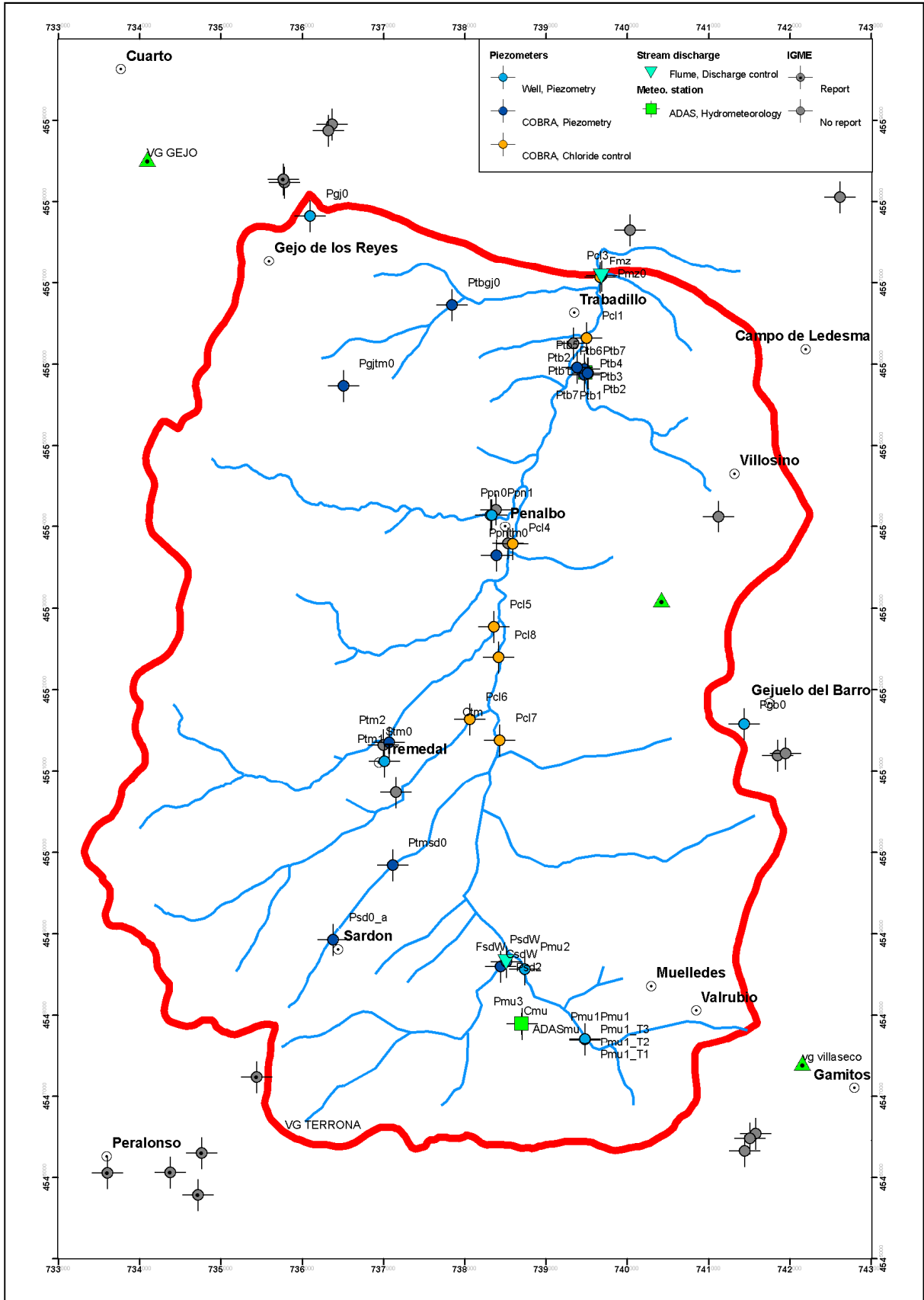


Figure 3-3: The monitoring network of piezometers in the Sardon Catchment

4. THEORETICAL BACKGROUND

An investigation of climate change effects on regional water resources consists of three steps (Xu, 1999): (1) using climate models to simulate climatic effects of increasing atmospheric concentration of greenhouse gases.

(2) Using downscaling techniques to link climate models and catchment-scale hydrological models or to provide catchment scale climate scenarios as input to hydrological models

(3) Using hydrological models to simulate hydrological impacts of climate change.

4.1. Climate Modeling

4.1.1. General Circulation Models

Studies of the impact of global warming on the hydrological cycles and water resources in the future usually rely on climate change scenarios projected by General Circulation Models (GCMs) (Chen *et al.*, 2006)

General circulation models (GCMs), also known as Global Climate Models refer to computer-driven models that use quantitative methods to simulate the interactions among the atmosphere, oceans and land surface. They are used for a variety of purposes ranging from the study of dynamics of the weather and climate system to the projections of future climate (Houghton *et al.*, 2001)

There are atmospheric and oceanic GCMs, for modelling the atmosphere and ocean respectively and the two can be combined to form an Atmosphere-Ocean Coupled General Circulation Model (AOGCM). These coupled models consist of four components namely atmosphere, land surface, ocean and sea ice. The resolution of the atmospheric part of the current AOGCM ranges from 2° to 10° latitude and longitude respectively and vertically from 10 to 30 layers.

4.1.2. Hadley Centre Coupled Model, version 3 (HadCM3)

The HadCM3, used in this study, is an example of a coupled atmosphere-ocean general circulation model (AOGCM), developed at the Hadley Centre in the United Kingdom. It has a horizontal resolution of 2.5°x3.75° (latitude x longitude) for the atmospheric component and 1.25°x1.25° for the oceanic component, giving a global grid of 96x73 grid points. It has 19 levels in the vertical (atmosphere) and 20 levels in the ocean.

4.1.3. Emission scenarios

Climate models' projections of future climate are dependent on the level of future greenhouse gas (GHG) and aerosol emissions. Since 2000 the emission scenarios used to make projections with climate models throughout the 21st century are called the SRES (Special Report on Emission Scenarios). They constitute a set of emission scenarios created by a group of world experts from the IPCC (Nakicenovic *et al.*, 2000) taking into account coherent hypothesis of the future evolution of world population growth, energy demand, efficient use of this or global economic growth among other considerations.

A scenario is a plausible future climate that has been constructed for explicit use in investigating the potential consequences of anthropogenic climate change...". (Houghton *et al.*, 2001).

Emission scenarios predict the emission of greenhouse gases, which are the main driving factors of the GCM predictions (O' Hare *et al.*, 2005).

There are 6 scenarios denoted as A2, B2, B1, A1B, A1T and A1F1 although A2 and B2 are the ones most simulated by AOGCMs. In this study only the A2 and B2 scenarios are considered, where the A2 scenario represents a future evolution of greenhouse gases that is increasing more rapidly than in the B2 scenario. These two scenarios are the ones most used in climate change projection studies.

Table 4-1: The Emission Scenarios of the IPCC Special Report on Emission Scenarios (SRES)

Scenario	Description
A1	Describes a future world of very rapid economic growth, global population that peaks in mid-century and declines thereafter, and rapid introduction of new and more efficient technologies. The A1 scenario family develops into three groups that describe alternative directions of technological change in the energy system. The three A1 groups are distinguished by their technological emphasis: fossil intensive (A1FI), non-fossil energy sources (A1T), or a balance across all sources (A1B; where balanced is defined as not relying too heavily on one particular energy source (a mix of fossil and non-fossil fuel).
A2	Describes a very heterogeneous world with continuously increasing global population and regionally oriented economic growth that is more fragmented and slower than in other storylines.
B1	Describes a convergent world with the same global population as in the A1 storyline but with rapid changes in economic structures toward a service and information economy, with reductions in material intensity, and the introduction of clean and resource-efficient technologies.
B2	Describes a world in which the emphasis is on local solutions to economic, social, and environmental sustainability, with continuously increasing population (lower than A2) and intermediate economic development. The scenario is oriented towards environmental protection but it focuses on local and regional levels.

4.1.4. Baseline Climate

This describes the present day climate and provides a reference to which future climates can be compared. The IPCC recommends that, where possible, 1961-1990 (the most recent 30-year climate 'normal' period) (Hulme *et al.*, 1995b; Kittel *et al.*, 1995) should be adopted as the climatological baseline period in impact and adaptation assessments. This period has been selected since it is considered to:

- be representative of the present-day or recent average climate in the study region
- be of a sufficient duration to encompass a range of climatic variations, including a number of significant weather anomalies
- cover a period for which data on all major climatological variables are abundant, adequately distributed over space and readily available
- include data of sufficiently high quality for use in evaluating impacts
- be consistent or readily comparable with baseline climatologies used in other impact assessments

4.1.5. Downscaling GCM output

With an average grid resolution of about 2.5° (~300km), GCMs are too coarse to be used for climate impact studies on regional and local scales as they are unable to resolve subgrid features such as clouds, topography and land use. There is therefore a need to downscale GCM output. Downscaling refers to obtaining finer resolution scenarios of climate change from the coarser resolution GCM output. As Fowler and Wilby, (2007) note, downscaling techniques, are commonly used to address the scale mismatch between coarse resolution global climate model (GCM) output and the regional or local catchment scales required for climate change impact assessment and hydrological modeling. To have confidence in a downscaling model and the results it produces it is important that the model should be able to reproduce observed past conditions (Wood *et al.*, 2004).

Generally there are two approaches to downscaling

- Dynamical downscaling
- Statistical downscaling

Dynamical Downscaling

Refers to the use of regional climate models (RCM) or limited-area models (LAM) which use the lateral boundary conditions from a GCM to produce high resolution outputs (Mearns *et al.*, 2003). RCM models are usually defined at a grid size of 10-50 km and are able to better represent topography and land use than GCM models (Sunyer *et al.*, 2010).

Statistical (Empirical) Downscaling

Statistical downscaling (SD) models rely on the fundamental concept that regional or local climate strongly depends on larger scale atmospheric variables (such as mean sea level pressure, geopotential height and wind fields).

The regional climate is considered to be conditioned by the large-scale climate through the relationship

$$R = f(X) \tag{4-1}$$

where:

R represents the local climate variable that is being downscaled (the predictand)

X is the set of large-scale climate variables (predictors) and

f is a function which relates the two and is typically established by training and validating the models using point observations or gridded reanalysis data .

According to (Wilby & Wigley, 1997), the following three implicit assumptions are involved in the statistical downscaling:

- Predictors are variables of relevance and are realistically modelled by the GCMs.
- The employed predictors fully represent the climate change signal.
- These observed empirical relationships are valid also under altered climate change conditions.

In addition, the predictors have to be physically and conceptually sensible with respect to the predictand and strongly and consistently correlated with the predictand.

Statistical downscaling methods can be divided into three main groups: regression models, weather generators and weather typing schemes.

Regression Models

Regression models are those that directly quantify a relationship between a local scale climate variable (predictand) and a set of large scale climate variables (predictors). Examples of regression models include artificial neural networks, principal components analysis, linear and non-linear regression and canonical correlation analysis.

Weather generators

A stochastic weather generator is a statistical downscaling process which produces artificial (synthetic) time series of weather data of unlimited length for a location. This synthetic data has similar statistical properties as the observed data used to calibrate the statistical model. In these models precipitation is generated first whilst the other variables such as minimum and maximum temperature, solar radiation and humidity are then modelled based on the occurrence of precipitation. The generation of precipitation is a two stage process with the first stage modelling the occurrence of a wet or dry day using a Markov procedure and the second stage focusing on the amount of precipitation.

Weather Typing/classification Schemes

Weather typing consists of classifying large-scale atmospheric circulation patterns into a finite number of discrete weather classes, which are then related to the local climate. Climate change is estimated by evaluating the change in the frequency of the weather classes simulated by the RCM or GCM (Fowlet *et al.*, 2007)

Table 4-2: Comparative summary of the relative merits of statistical and dynamical downscaling techniques (adapted from Wilby and Wigley, 1997).

Statistical downscaling	Dynamical downscaling
<p>Advantages</p> <ul style="list-style-type: none"> ▪ Comparatively cheap and computationally efficient ▪ Can provide point-scale climatic variables from GCM-scale output ▪ Can be used to derive variables not available from RCMs ▪ Easily transferable to other regions ▪ Based on standard and accepted statistical procedures ▪ Able to directly incorporate observations into method <p>Disadvantages</p> <ul style="list-style-type: none"> ▪ Require long and reliable observed historical data series for calibration ▪ Dependent upon choice of predictors ▪ Non-stationarity in the predictor-predictand relationship ▪ Climate system feedbacks not included ▪ Dependent on GCM boundary forcing; affected by biases in underlying GCM ▪ Domain size, climatic region and season affects downscaling skill ▪ Choice of empirical transfer scheme affects results 	<p>Advantages</p> <ul style="list-style-type: none"> ▪ Produces responses based on physically consistent processes ▪ Produces finer resolution information from GCM-scale output that can resolve atmospheric processes on a smaller scale ▪ Resolve atmospheric processes such as orographic precipitation ▪ Consistency with GCM <p>Disadvantages</p> <ul style="list-style-type: none"> ▪ Computationally intensive ▪ Limited number of scenario ensembles available ▪ Strongly dependent on GCM boundary forcing ▪ Choice of domain size and location affects results ▪ Initial boundary conditions affect results ▪ Choice of cloud/ convection scheme affects (precipitation) results ▪ Not readily transferred to new regions or domains

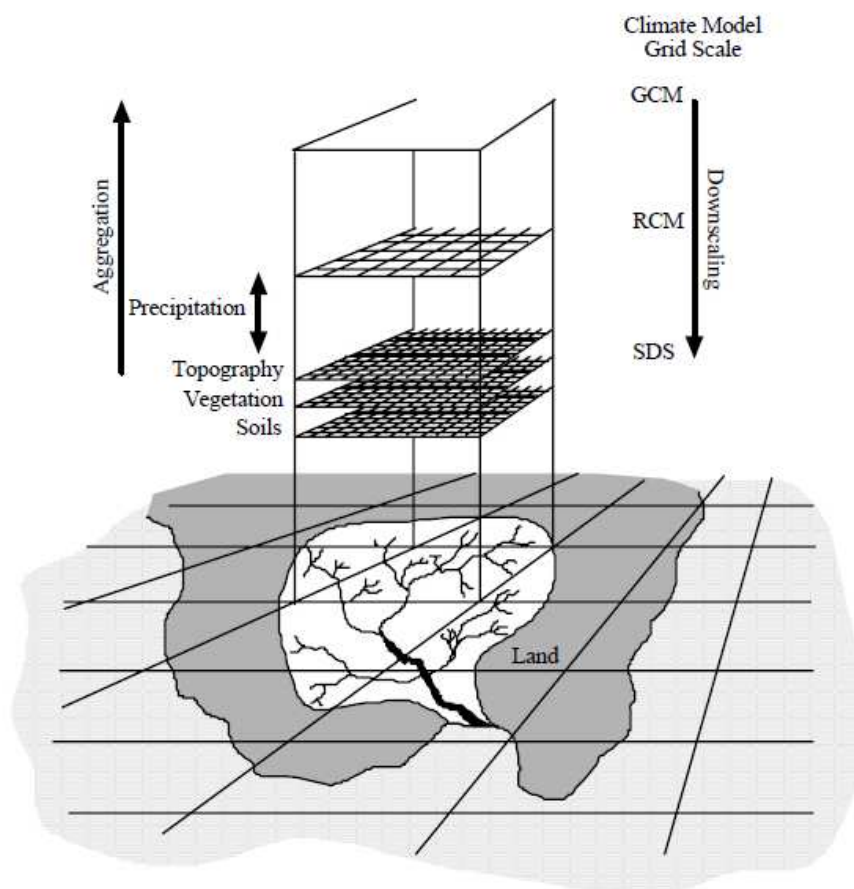


Figure 4-1: A schematic illustrating the general approach to downscaling. (Adapted from Wilby and Dawson 2007)

4.1.6. Statistical Downscaling Model (SDSM)

In this study statistical downscaling is used to downscale climate change scenarios using the Statistical DownScaling Model (SDSM). The Statistical Downscaling Model (SDSM) is a decision support tool, developed by Robert Wilby and Christian Dawson (Wilby *et al.*, 2002) in the UK, for assessing local climate change impacts using a robust statistical downscaling technique. It permits the spatial downscaling of daily predictor-predictand relationships using multiple linear regression techniques. SDSM is best categorised as a hybrid of the stochastic weather generator and regression-based downscaling methods (Wilby & Wigley, 1997).

The downscaling of daily weather series is divided into seven steps:

1. Quality control and data transformation;
2. Screening of the predictor variables;
3. Model calibration;
4. Weather generation using observed predictors;
5. Statistical analyses;
6. Graphing of model output;
7. Scenario generation using climate model predictors

Quality control and data transformation

Quality control check enables the identification of data errors and the specification of missing data codes and outliers before model calibration. The regression technique used in SDSM assumes that the input data has a normal distribution such as the case with temperature. Where the data is skewed (e.g. precipitation) then a transformation of the data is necessary.

Screening of the predictor variables

This stage identifies the large scale predictor variables which are significantly correlated with observed station (predictand) data through seasonal correlation analysis, partial correlation analysis and scatter plots. The predictands considered in this study are precipitation, maximum and minimum temperature. Precipitation is modelled as a conditional process that depends on other intermediate process like the occurrence of humidity, cloud cover, and /or wet-days whereas temperature is an unconditional process.

Predictor data files for SDSM were obtained from the Canadian Institute for climate studies (CICS) website. <http://www.cics.uvic.ca/scenarios/sdsm/select.cgi>.

The predictors are available on a grid box basis of the same latitude and longitude as the HadCM3 model. Once the coordinates closest to the study area are specified, the predictors which are in three directories are extracted. In this study the coordinates closest to the study area, Trabadillo were specified as 40°N and 352.5°E.

NCEP_1961-2001:

This directory contains 41 years of daily observed predictor data, derived from the National Centres for Environmental Prediction (NCEP) reanalyses, normalised over the complete 1961-1990 period.

H3A2a_1961-2099:

This directory contains 139 years of daily GCM predictor data, derived from the HadCM3 A2(a) experiment, normalised over the 1961-1990 period.

H3B2a_1961-2099:

This directory contains 139 years of daily GCM predictor data, derived from the HadCM3 B2(a) experiment, normalised over the 1961-1990 period.

Table 4-3: Large-scale atmospheric variables from the NCEP reanalysis and HadCM3 simulation

	Predictor	Description		Predictor	Description
1	mslpeu	mean sea level pressure	14	P5_zheu	500hpa divergence
2	p_feu	surface air flow strength	15	p8_feu	850hpa airflow strength
3	p_ueu	surface zonal velocity	16	p8_ueu	850hpa zonal velocity
4	p_veu	surface meridian velocity	17	p8_veu	850 hpa meridional velocity
5	p_zeu	surface vorticity	18	p8_zeu	850 hpa vorticity
6	p_theu	surface wind direction	19	p850eu	850hpa geo-potential height
7	p_zheu	surface divergence	20	p8theu	850hpa wind direction
8	p5_feu	500hpa air flow strength	21	p8zheu	850 hpa divergence
9	p5_ueu	500pa zonal velocity	22	r500eu	relative humidity at 500hpa
10	p5_veu	500hp meridional velocity	23	r850eu	relative humidity at 850hpa
11	p5_zeu	500hpa voritcity	24	rhumeu	near surface relative humidity
12	p500eu	500hpa geo-potential height	25	shumeu	surface specific humidity
13	p5theu	500hpa wind direction	26	tempeu	mean temperature at 2 m

All predictors, except the wind direction were normalized with respect to the 1961-1990 mean and standard deviation.

Model Calibration

This process constructs the downscaling models based on multiple linear regression equations given the daily predictand data and the regional scale atmospheric predictor variables chosen in the screening of predictor variables stage. A choice is made whether individual downscaling models will be calibrated for each month, season or year. The calibration algorithm gives the percentage of explained variance (R^2) and standard error (SE) for each regression model type (monthly, seasonal or annual average).

Weather Generator

Involves the generation of synthetic daily weather series representative of current climate conditions using the calibrated models and daily observed or reanalysis atmospheric predictor variables. The calibrated models can be validated by using them with the independent data excluded from the calibration process. There is need to specify how many ensembles of synthetic data are required with up to a max of 100 being possible. Each ensemble member is considered to be an equally plausible representation of local climate resulting from using the same set of predictor variable in the calibrated models.

Analyse data

SDSM provides basic descriptive statistics for both downscaled scenarios and observed climate data. A particular ensemble member or the mean can be analysed.

Graphical Analysis

Graphical analysis is achieved through the use of three options: frequency analysis, compare results and time series analysis screens.

Scenario generation

The scenario generation operation produces ensembles of synthetic daily weather series given the regression weight produced during calibration process and the daily atmospheric predictor variables supplied by a GCM (either under the present or future greenhouse gas forcing).

4.2. Hargreaves Equation

One of the inputs into the pyEARTH model is potential evapotranspiration (PET). A number of methods are available for calculating PET. In this study the Hargreaves method is used to compute this parameter.

Hargreaves equation is given by:

$$ET_o = 0.0023R_a(T_a + 17.8)\left(\sqrt{T_{\max} - T_{\min}}\right) \quad (4.1)$$

where

- ET_o is reference crop evapotranspiration (mm/day)
- T_a is the daily mean air temperature (°C) i.e.

$$T_a = \frac{(T_{\max} + T_{\min})}{2} \quad (4.2)$$

T_{\max} is the daily maximum temperature (°C)

T_{\min} is the daily minimum temperature (°C)

R_a is extraterrestrial radiation ($\text{MJm}^2 \text{day}^{-1}$) and is given by

$$R_a = \frac{24(60)}{\pi} G_{sc} dr [\omega_s \sin \varphi \sin \delta + \cos \varphi \cos \delta \sin \omega_s] \quad (4.3)$$

The corresponding equivalent evaporation in mm day^{-1} is obtained by multiplying R_a by 0.408, i.e. $1\text{MJm}^2\text{day}^{-1} = 0.408\text{mmday}^{-1}$

- i) G_{sc} is the solar constant = $0.082\text{MJ}/\text{m}^2\text{min}$
- ii) dr is the inverse relative distance(Earth-Sun)

$$dr = 1 + 0.033 \cos\left(\frac{2\pi J}{365}\right) \quad (4.4)$$

J is the Julian day (i.e. the number of the day in the year between 1 (1 January) and 365 or 366 (31 December))

iii) ω_s is the sunset hour angle and is given by

$$\omega_s = \arccos[-\tan \varphi \tan \delta] \quad (4.5)$$

iv) δ is the solar declination, given by

$$\delta = 0.409 \sin\left(\frac{2\pi J}{365 - 1.39}\right) \quad (4.6)$$

v) φ is the latitude (radians). Latitude, φ is positive in the northern hemisphere and negative in the southern hemisphere.

4.3. Groundwater recharge modeling with py EARTH 1-D MODEL

Groundwater recharge can be defined as the downward flow of water reaching the water table from the unsaturated zone (Freeze and Cherry, 1979; Lerner *et al.*, 1990) .A number of factors affect groundwater recharge and these include vegetation type, land use, soil type, the antecedent moisture condition of the soil profile, depth to the water table, aquifer properties and the rate, timing and duration of irrigation or rainfall.

4.3.1. Methods of estimating recharge

In arid and semi arid areas where recharge rates are generally low compared to annual rainfall or evapotranspiration, the estimation of recharge is particularly important for water management decisions. Equally important is the estimation of future recharge rates because of the impact of envisaged climate change and increased demand for groundwater resources in the future (Kirchner, 2003).

There are a number of recharge methods in use and these differ in terms of data needs, ease of use and the associated cost. The choice of appropriate methods for a recharge study requires the considerations of several factors such as the goal of the recharge study, the required accuracy and reliability, space and time scale, the range of the expected recharge estimates, the time to be spent on the study, and the financial resources available (Scanlon *et al.*, 2002; Lerner *et al.*, 1990).

Two broad groups of recharge estimation can be identified:

Direct methods

These consider percolation, soil moisture distribution and evapotranspiration to estimate recharge. They include physical balance methods, empirical balance methods, unsaturated zone models and tracer methods.

Indirect methods

The recharge to a groundwater aquifer cannot be easily measured directly, and is usually estimated by indirect means (Lerner *et al.*, 1990). Indirect methods consider fluctuations of groundwater table as an indicator of recharge and include:

- Parametric balance methods which describe the relationship between groundwater table and recharge with two or more parameters.
- Physical methods which use physical processes of saturated flow to obtain recharge estimates.

4.3.2. EARTH MODEL

The Extended model for Aquifer Recharge and soil moisture Transport through the unsaturated Hard rock (EARTH) is a 1D lumped parameter hydrological model for the simulation of recharge and groundwater level fluctuations developed by (Lee & Gehrels, 1990). Its inputs include:

- Meteorological data (daily precipitation and potential evapotranspiration)
- Hydrological data (daily groundwater level data used for model calibration)
- Input values for model parameters

As output the model gives actual evapotranspiration, aquifer recharge, groundwater levels, precipitation excess, ponding, surface runoff and soil moisture.

In this study a modified version of the EARTH model, the pyEARTH-1D model (Frances, 2008) is used to estimate recharge. It has a graphical user interface (GUI) that allows the user to input data easily and uses simple ASCII file as input and output.

Background Information

The EARTH model combines both direct and indirect methods of recharge measurement and consists of four sequential modules or reservoirs, MAXIL (Maximum Interception Loss), Soil moisture Storage (SOMOS), LINRES (Linear Reservoir Routing) and SATFLOW (Saturated Flow), each performing a particular function and representing a specific zone in the recharge process. The direct part determines recharge using physical processes above the groundwater table and the indirect part calculates the groundwater level with the estimated recharge of the direct part.

The first two modules, MAXIL and SOMOS, represent the agro-hydrometeorological zone while LINRES and SATFLOW, represent the hydrogeological zone of the modelled space.

The model is calibrated using measured groundwater levels and/or soil moisture values.

The advantage of the EARTH model is its simplicity and insensitivity to the type of recharge mechanism (Healy & Cook, 2002). However it does not account for lateral groundwater flow in recharge evaluation.

MAXIL

This module calculates the amount of precipitation intercepted by vegetation, depression storage and loss to evaporation. The effective rainfall or precipitation excess (P_e), i.e. the fraction of precipitation which reaches the surface and infiltrates is given by

$$P_e = P - MAXIL - E_o \quad (4.7)$$

P is precipitation

$MAXIL$ is the intercepted fraction of P

P_e is precipitation excess

E_o is surface evaporation

SOMOS

This module distributes infiltration water into actual evapotranspiration, percolation and surface storage and/or runoff. The remaining part is thus the change in soil moisture storage. It is a water balance module in the root zone.

The equation of soil moisture storage variation in the root zone is

$$\frac{dS}{dt} = P_e - ET_a - R_p - E_o(SUST) - Q_s \quad (4.8)$$

where

S is soil moisture

P_e is precipitation excess

ET_a is actual evapotranspiration

R_p is percolation

$SUST$ is ponding water

Q_s is surface runoff

$\frac{dS}{dt}$ is change in storage

$E_o(SUST)$ is evaporated fraction of ponding water

The soil moisture S is defined as:

$$S = WD \quad (4.9)$$

W is volumetric soil moisture content

D is thickness of the soil layer where soil moisture changes occur

The actual evapotranspiration ET_a is obtained from

$$ET_a = PET \cdot \left(\frac{\theta - \theta_{pwp}}{\varphi - \theta_{pwp}} \right) \quad (4.10)$$

where

PET is potential evapotranspiration

θ is actual volumetric soil moisture

θ_{pwp} is the permanent wilting point

φ is porosity

The percolation (R_p) is given by

$$R_p = K \cdot \left| \frac{d_{hp}}{dz} + 1 \right| \approx K_{sat} \left(\frac{\theta - \theta_{fc}}{\varphi - \theta_{fc}} \right) \quad (4.11)$$

where

K is the unsaturated hydraulic conductivity

$\frac{dh_p}{dz}$ is the gradient of the hydraulic potential (positive downward)

K_{sat} is the saturated hydraulic conductivity

θ is the actual volumetric soil moisture

θ_{fc} is the soil moisture at field capacity

φ is the porosity

It is assumed in the simplification of the above equation that percolation is equal to the unsaturated hydraulic conductivity.

SUST

SUST (Surface storage) is the module that calculates the amount of water that accumulates when maximum percolation is reached and is lost to evaporation or added once again to precipitation excess. If the amount of water in SOMOS reaches saturation, and the infiltration rate exceeds percolation rate R_p , surface ponding may occur. In this case

$$\frac{d(SUST)}{dt} = P_e - ET_a - R_p - E_o \quad (4.12)$$

$SUST$ is the ponding water

E_o is the open water evaporation

If the ponding water exceeds a threshold value ($SUST_{max}$), that represents the maximum surface storage capacity, runoff (Q_s) will occur i.e.

$$Q_s = SUST - SUST_{max} \quad (4.13)$$

LINRES

This is the module that controls the time that percolating water (recharge) takes to reach the groundwater table due to its depth. It is a module for the unsaturated zone that is programmed by a transfer function that redistributes percolation temporally between the soil reservoir SOMOS and the SATFLOW module. Moisture which is percolating down from the soil reservoir can no longer be lost by evaporation. However, the groundwater table may be further down and therefore there is a delay before the soil moisture actually reaches the water table. This delay is modelled by linear reservoirs (Gieske, 1992).

The equations to delay R_p in recharge are:

$$R = Y_n = \frac{f}{1+f} \sum_{i=0}^n (1+f)^{-i} Y_{n-i}^* \quad (4.14)$$

$$Y_o = \frac{1+f}{f} R_p \quad (4.15)$$

where

R is recharge

f is unsaturated recession constant

n is the number of reservoirs

Y^* refers to results from the previous time step

Y_0 is the upper boundary condition

R_p is the percolation

SATFLOW

This is the module that calculates groundwater level rise using the recharge, or in its absence, it calculates the groundwater recession.

The equation to determine groundwater level fluctuation is:

$$\frac{dh}{dt} = \frac{R}{STO} - \frac{h}{RC} \quad (4.16)$$

where

R is the recharge

STO is storage coefficient

RC is the saturated recession constant

h is the groundwater level above the local base level

FLOWCHART OF EARTH MODEL

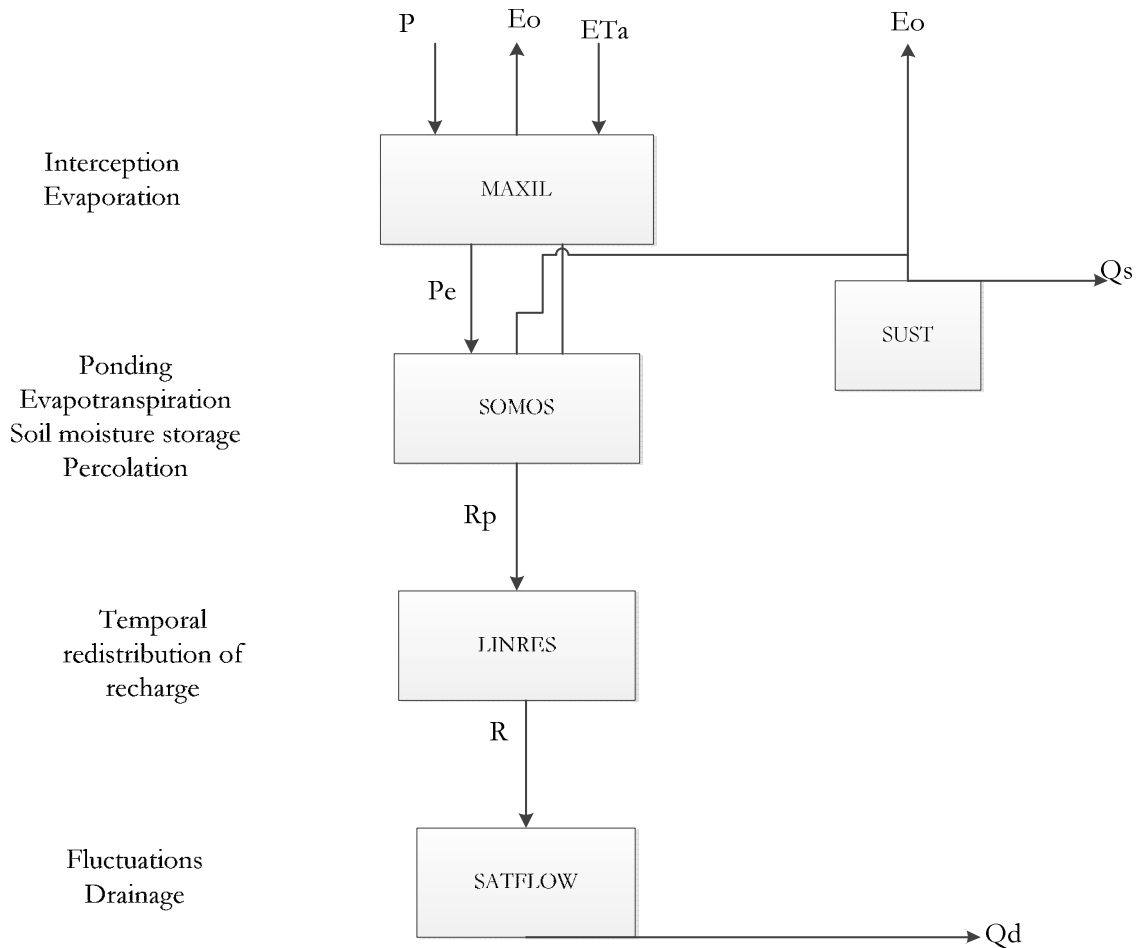


Figure 4-2: EARTH-1D Model flowchart. Source :(Lee & Gehrels, 1990)

- P is precipitation
- Pe is precipitation excess
- Eo surface evaporation
- ETa is actual evapotranspiration
- Qs is surface runoff
- Rp is percolation
- R is recharge
- Qd is subsurface drainage

Table 4-4: Parameter configuration for the EARTH Model

Model	Parameter	Symbol	Source
MAXIL	Maxil		Field observation and literature
SOMOS	Maximum Soil moisture content	Sm	Laboratory analysis of soil samples
	Residual soil moisture content	Sr	
	Initial Soil Moisture content	Si	
	Soil moisture at field capacity	Sfc	
	Maximum Surface Storage	SUSTmax	
	Saturated Conductivity	Ks	
LINRES	Unsaturated recession constant	f	Groundwater level data
	Number of reservoirs	n	Field observation
SATFLOW	Saturated recession constant	RC	Groundwater level fluctuations
	Storage coefficient	STO	Previous studies in study area
	Initial groundwater level	Hi	Groundwater level data from
	Local base level	Ho	measured groundwater fluctuations

4.4. Groundwater modeling

Groundwater modelling involves the use of computer generated models in the prediction of the flow of water. In this study MODFLOW (McDonald & Harbaugh, 1988) was used to simulate groundwater flow. MODFLOW is a block centred 3D finite difference groundwater flow model that can simulate a number of different types of aquifers. It consists of a series of packages with each package performing a specific function.

A groundwater modelling process consists of two steps:

- Conceptual model
- Numerical model

4.4.1. Conceptual model

According to (Anderson & Woessner, 1992) a conceptual model is a simplified but accurate representation of the field groundwater flow system shown as a cross section or block diagram.

In defining the conceptual model, the hydrostratigraphic units, preliminary water balance, model boundaries, flow system, direction and flow rate and model boundaries need to be specified.

4.4.2. Numerical Model

This is a mathematical model described by some governing equations, with associated boundary and initial conditions. It expresses the conceptual model in mathematical terms. The solution of the mathematical model yields the required predictions of the real-world system's behaviour in response to various sources and/or sinks. The governing equation for groundwater flow in 3D is based on the law of mass balance and Darcy's law (see equation 1.2).

Numerical groundwater modelling can be performed in steady state or transient state conditions. Fluxes are constant during the simulation period in steady state whilst they vary both in space and time in fully transient modeling.

3D groundwater flow through a porous medium is governed by the following equation:

$$\frac{\partial}{\partial x} \left(K_x \frac{\partial h}{\partial x} \right) + \frac{\partial}{\partial y} \left(K_y \frac{\partial h}{\partial y} \right) + \frac{\partial}{\partial z} \left(K_z \frac{\partial h}{\partial z} \right) = S_s \frac{\partial h}{\partial t} - W \quad (4.17)$$

where

- K_x, K_y, K_z are values of hydraulic conductivity along the x, y and z axes,
- h is the hydraulic head,
- W is flux per unit volume, representing sinks and/or sources of water
- S_s is specific storage of the aquifer

5. METHODOLOGY

5.1. Generating climate time series

Rainfall and temperature measurements taken at Trabadillo show that these two are uniform at catchment scale since the catchment is small and with more or less uniform topography. The Trabadillo rainfall and temperature are therefore taken as representative of the catchment in this study. There are a number of gaps however in the historical temperature and precipitation data of Trabadillo. Since climate change studies require the analysis of long data series the precipitation data gaps were therefore filled using an interpolation method, the Normal Ratio method (Villazón & Willems, 2010). Seven neighbouring AEMET stations used for the interpolation are Villaseco, Ledesma, Villaseco Reyes, Salamanca, Manzano, Villamuerto and Villar de Peralonso (Figure 5-1).

The equation for the normal ratio method is:

$$\frac{P_x}{N_x} = \frac{1}{n} \left(\frac{P_1}{N_1} + \frac{P_2}{N_2} + \dots + \frac{P_N}{N_N} \right) \quad (5.1)$$

where

- P_x is the missing precipitation value for station X
- P_1, P_2, \dots, P_n are precipitation values at adjacent stations for the current period
- N_x is the long-term, annual average precipitation at station X
- N_1, N_2, \dots, N_n is the long-term precipitation for neighboring stations
- n is the number of adjacent stations

Only two AEMET stations, Salamanca and Villamuerto had records of minimum and maximum temperature. To fill in temperature gaps at Trabadillo a correlation using data for a common period, 2004 to 2008 was made. The correlations of Trabadillo minimum temperatures with Villamuerto and Salamanca gave R^2 values of 0.29 and 0.68 respectively while maximum temperatures gave R^2 values of 0.47 and 0.84 respectively. The gaps were then filled with Salamanca data using the nearest neighbor approach (Eischeid *et al.*, 2010) However due to some inconsistencies and obvious errors in Trabadillo temperature data, that data could not be relied upon. The Salamanca complete records were therefore used to represent Trabadillo temperature since the correlations were relatively high. The figure below shows the spatial distribution of the areas used in the interpolation relative to the position of Trabadillo.

Figure 5-1 below shows the spatial distribution of the stations used for generating climate time series for Trabadillo.

5.3. Statistical Downscaling

Future climate output of daily precipitation and temperature from the general circulation model (GCM), the Hadley Centre Coupled Model, version3 (HadCM3) was downscaled using a statistical method. The downscaling was done to ensure that the output of the GCM matched the spatial resolution of the catchment.

The Statistical DownScaling Model (SDSM) was used in the downscaling of the baseline period and future for two emission scenarios, A2 and B2. The SDSM was chosen because it is simple to use and can provide local point-scale climatic variables from GCM-scale output, which is required in climate change impact studies of this nature. It can also read data from HADCM3 model output directly. On the other hand the HadCM3 is widely used in climate impact studies and simulates the two emission scenarios A2 (medium-high) and B2 (medium – low) analysed in this study.

The future simulations were divided into three 30 year periods namely the 2020s (2010-2039), 2050s (2040-2069) and 2080s (2070-2099) based on the mean of 20 ensembles which was then used for analysis purposes. To evaluate the performance of the downscaling, the mean of the downscaled data was compared with observed data.

a) Parameter Settings in SDSM downscaling

The following settings were adopted for the downscaling of precipitation and temperature.

Model Transformation

The fourth root transformation was used for downscaling precipitation while the default (None) was used for temperature.

Event Threshold

This parameter was set at 0.1mm/ day during the calibration of daily precipitation to treat trace rain days as dry days. For temperature it was set at 0.

Variance Inflation

This controls the amount of variance in downscaled daily weather variables, with larger values increasing the variance of downscaled properties.

Bias Correction

Compensates for any tendency to overestimate or underestimate the mean of conditional processes by the downscaling model. Different values of bias correction and variance inflation adjustment were tried and the best combination of these parameters gave a calibrated model with maximum coefficient of determination (R^2), minimum standard error (SE) and identical standard deviation in the comparison of observed and simulated data.

b) Model Calibration

The SDSM model was calibrated for each month for precipitation, minimum and maximum temperature using the set of selected NCEP predictors and observed data. The goodness of a calibration is measured by values of the percentage of explained variance (R^2) and standard error (SE). Results of the calibration indicating specific predictors used for downscaling each parameter are indicated in Figure 5-1.

c) Predictors

During the Screen Variables stage of SDSM downscaling the following predictors were chosen

Table 5-1: Large scale predictor variables selected for SDSM downscaling

	Large scale predictor	Precipitation	Minimum Temperature	Maximum Temperature
ncepp_veu	Surface meridian velocity	✓		
ncepp_zeu	Surface vorticity	✓		✓
ncepp_ueu	Surface zonal velocity	✓		✓
ncepp_feu	Surface air flow strength			
ncepp_zheu	Surface divergence		✓	
ncepp5_zeu	500hPa vorticity	✓		
ncepp5_veu	500hPa meridional velocity		✓	✓
ncepp500eu	500hPa geopotential height			✓
ncepp8_ueu	850hPa zonal velocity	✓		
ncepp8_veu	850hPa meridional velocity		✓	
ncepp8_feu	850hPa airflow strength		✓	✓
ncepp8_zeu	850hPa vorticity			✓
ncepp8theu	850hPa wind direction			
ncepr500eu	Relative humidity at 500hPa	✓		
ncepr850eu	Relative humidity at 850hPa		✓	
ncepshumeu	Surface specific humidity	✓	✓	
nceprhumeu	Near surface relative humidity	✓		
nceptempeu	Mean temperature at 2m		✓	✓

d) Validation

To evaluate the performance of any downscaling process it is important that the synthesized data should closely replicate observed data. Usually part of the observed data series is used for calibrating the model while the data which was not used for calibration is used for independent model verification. In this study data for 1961 -1975 was used for calibrating the model while the data for 1976-1990 was used for model validation.

e) Downscaling present (observed) climate

SDSM was used to downscale the present climate (1961-1990) using NCEP and HadCM3 A2 and B2 predictors. The results obtained were then compared with the observed values.

f) Downscaling future climate

The future climate was downscaled using the HadCM3 predictors. Changes in mean daily precipitation and temperature were analysed for the 2020s, 2050s and 2080s for the A2 and B2 scenarios by comparing with the baseline period (1961 to 1990).

Output of the downscaling process, daily temperature and precipitation provided input into the hydrologic model, pyEARTH 1-D.

5.4. Converting climate model output into groundwater recharge

Daily temperature from the downscaling process was converted into daily potential evapotranspiration using Hargreaves method and this, together with daily precipitation provided the input into pyEARTH-1D recharge model. The choice of the pyEARTH 1-D model was influenced by its success in other studies. In a study on soil moisture dynamics and evapotranspiration (Obakeng, 2007), the EARTH model was used to estimate annual recharge in the Serowe area, a semi arid area in Botswana. Results obtained were of the same order of magnitude with those obtained using a water table Fluctuation Model (WTF) and a Linear Reservoir approach (LINRES). The Hargreaves method was used because of its simplicity since it uses information on daily temperature and the latitude of the place only to calculate potential evapotranspiration and is therefore suitable in areas where data is scarce. A study by (Trajković & Gocić, 2010) comparing six methods to calculate PET at an area with a semi arid Mediterranean climate in southern Italy showed that the Hargreaves formula produced results comparable to the widely used Penman Monteith formula.

The pyEARTH 1-D recharge model was calibrated with groundwater level and soil moisture data for 2004 to 2008 and June 2008 to December 2008 respectively. The calibrated model was used to estimate recharge and actual evapotranspiration for the historical (1961 -1990) and forecast periods (2010-2039) for both the A2 and B2 scenarios.

5.5. Groundwater Modeling

5.5.1. Model Set up and boundaries

In the Sardon catchment, two layers underlain by a massif granite basement can be identified. The major groundwater flow direction is S-N, being controlled by topography and subsurface structures in the catchment.

Boundary conditions are mathematical statements which specify the head or fluxes at the boundaries of the model domain. The correct assignment of the boundaries is important since it controls the flow regime of the numerical model (Dua, 1999). No flow boundary conditions were assigned along all the external boundaries of the catchment. Sardon river which flows along the major fault zone is simulated by drain boundary condition in which the drain elevation is selected bottom of the river. The site was simulated as two layered structure with upper layer unconfined and lower layer confined. The grid size of the model is 100 m x 100m and covers the whole area of the Sardon catchment giving 131 rows and 95 columns.

5.5.2. Model Calibration

The groundwater flow model was calibrated from 2004 to 2008 using data from 5 piezometers. During the calibration the differences between measured and simulated piezometric heads were initially minimized by trial and error adjustment of the hydraulic conductivities using the calibrated model of Rajapakse(2009) as a starting point. Later the automated parameter estimation, PEST was applied to optimize the hydraulic conductivities and the main storage parameters of specific yield and storage coefficient. Results of the calibration and simulations are shown in chapter 6. The model grid with the 5 piezometers used for calibration is shown in Fig 4-3 below. The yellow structure is the Sardon river.

The calibrated model was then run in transient state to estimate groundwater resources for the A2 and B2 future scenarios for the period 2010-2039 after applying uniform recharge over the whole catchment.

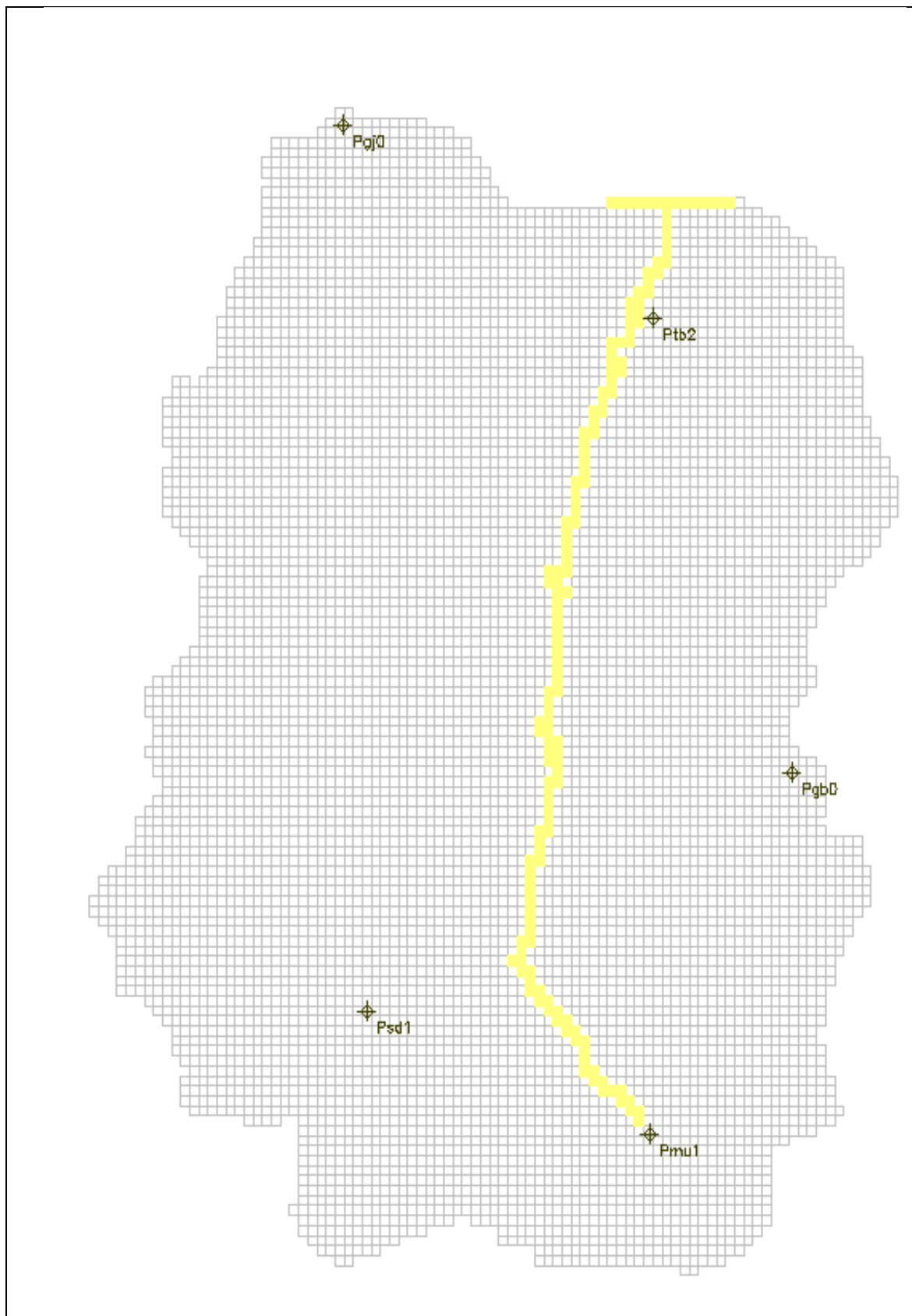


Figure 5-2: Model layer 2 and the 5 calibration piezometers

5.5.3. Time Discretization

A stress period can be defined as a period which represents a uniform groundwater flow regime and is defined within the individual simulation periods of the groundwater model. The stress periods were defined after considering the temporal variability of rainfall and recharge computed from the pyEARTH 1-D model. Determining the simulation time steps in transient modelling is a critical step in model design since values of space and time discretization strongly influence the numerical results (Anderson & Woessner, 1992). The 30 year simulation period from Jan 2010 to Dec 2039 was divided into 60 stress periods of 240 and 120 days. These were in turn divided into time steps of 8 and 4 months respectively. The stress periods and time steps for simulating transient flow are shown in appendix 2.

The selected stress periods can be divided into two groups:

- Wet winter season (Oct to May)
- Dry summer season (June to Sept)

5.5.4. Water balance

The water balance or budget is a quantitative statement of the balance between water gained by the catchment and water losses from the catchment during a specified period. Recharge, groundwater storage and outflow through drain package constitute the major components of the water balance in the study area and all these were calculated for each stress period. Appendix 3 shows the total water balance for all the stress periods.

6. RESULTS AND DISCUSSION

6.1. Generating climate time series

The graphs below show the generated time series of annual precipitation, mean annual minimum temperature, mean annual maximum temperature and mean annual average temperature using interpolation means.

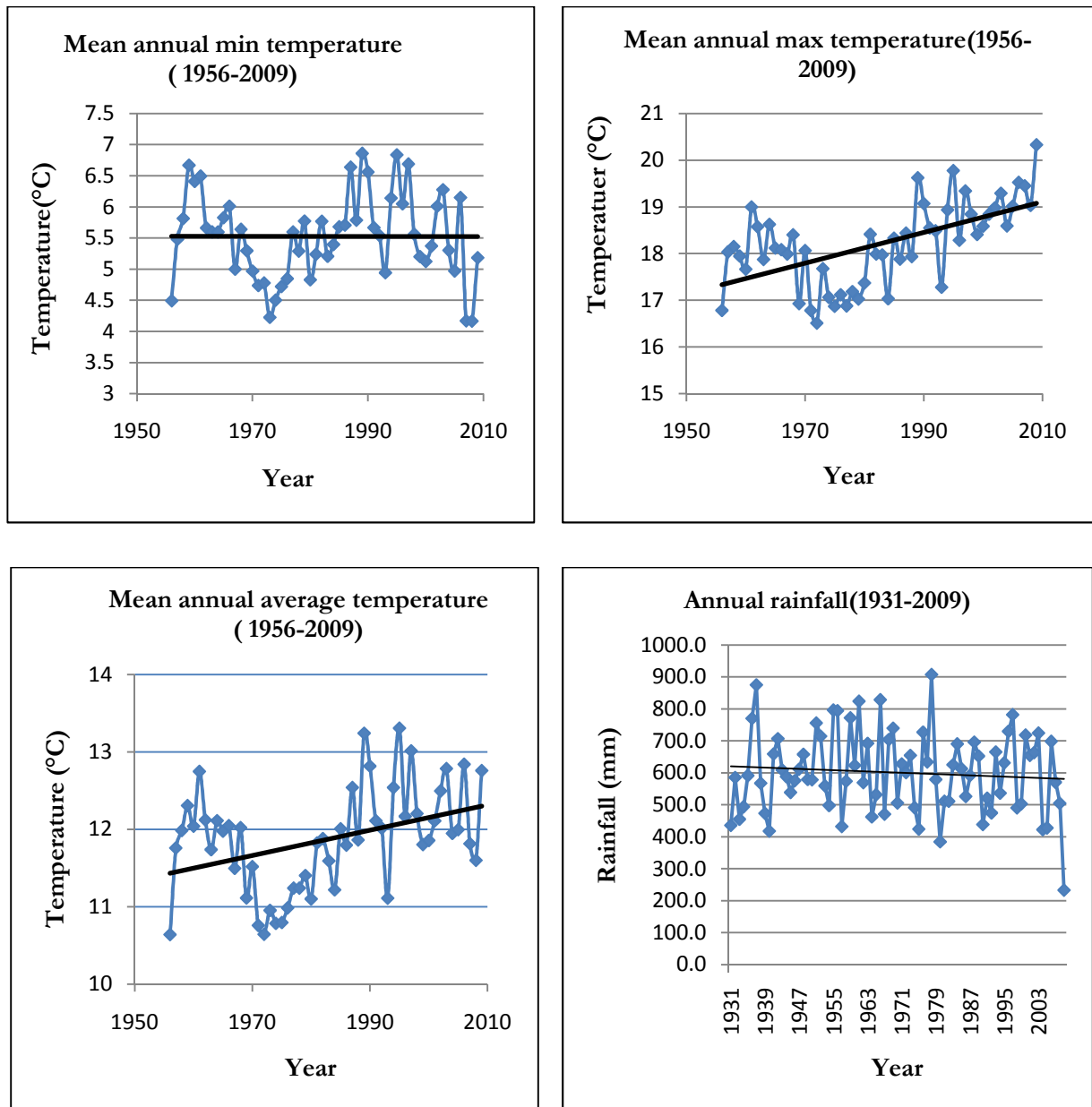


Figure 6-1: Time series of precipitation and temperature for Trabadillo station

6.2. Trend Analysis

Table 6-1: Trend testing results

TEST	PARAMETER			
	Precipitation	Mean annual Min temperature	Mean annual Max temperature	Mean annual Average temperature
Mann-Kendall	NS	NS	S (0.01)	S (0.05)
Spearman's Rho	NS	NS	S (0.01)	S (0.01)
Linear regression	NS	NS	S (0.01)	S (0.01)
Cusum	NS	NS	S (0.01)	S (0.05)
Cumulative deviation	NS	NS	S (0.01)	S (0.01)
Worsley likelihood	S (0.1)	NS	S (0.01)	S (0.01)
Rank Sum	NS	NS	S (0.01)	S (0.01)
Student's t	NS	NS	S (0.01)	S (0.05)
Median Crossing	NS	S (0.05)	S (0.01)	S (0.01)
Turning Point	NS	S (0.05)	NS	NS
Rank Difference	NS	S (0.01)	S (0.01)	S (0.01)
Auto Correlation	NS	S (0.01)	S (0.01)	S (0.01)

(NS means not significant at $\alpha = 0.1$; S means statistically significant, with the significance level shown in brackets).

Results of the analysis in Table 6-1 above indicate that maximum and average temperature showed a significant increasing trend for the period under consideration. Mean annual average temperatures and mean annual maximum temperatures increased by 0.21°C and 0.38°C respectively relative to the baseline period. Mean annual minimum temperature and precipitation however showed no significant trend.

6.3. Downscaling GCM Output

a) Model calibration

The results of calibration indicate that values of R^2 were greater for temperature than for precipitation. This indicates the difficulty in finding significant climate variables from the NCEP data that could explain well the variability of daily precipitation. Nguyen et al. In general daily precipitation amounts at individual sites are poorly resolved by regional scale predictors. (Doyle, 1997) notes that both the rain occurrence and the amount of precipitation are stochastic processes which make the downscaling of precipitation a difficult problem.

These results are however comparable to those obtained by other researchers elsewhere. In a study to test the ability to simulate daily precipitation and extreme temperature series for four stations in the Montreal region in Quebec (Nguyen, *et al.*, 2004), two downscaling methods, the LARS-WG and SDSM were compared. Values of R^2 obtained were 0.714 and 0.785 for maximum and minimum temperatures respectively. The values for precipitation ranged from 0.062 to 0.098.

Table 6-2: Model calibration results

	Precipitation	Minimum temperature	Maximum Temperature
R ²	0.143	0.678	0.777
Standard Error(SE)	0.303	1.817	1.853
Variance Inflation	12	12	12
Bias Correction	0.915	1	1

b) Validation

The mean daily precipitation and temperature were used to test model performance during the validation period. The results are shown in the graphs below.

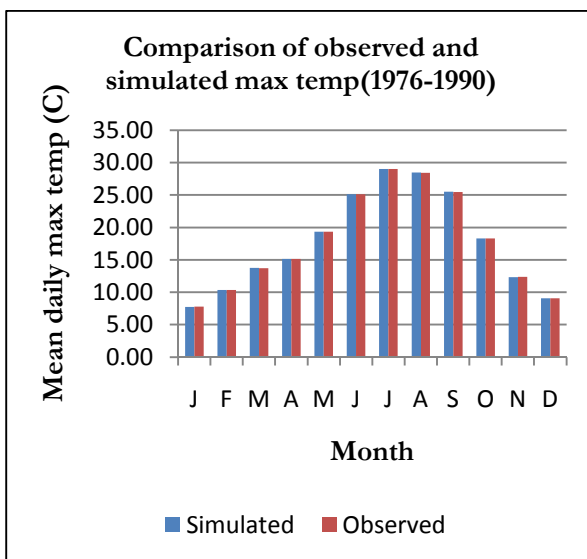
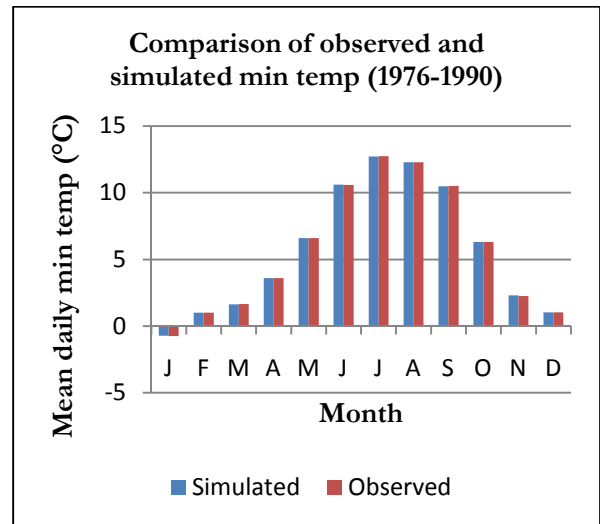
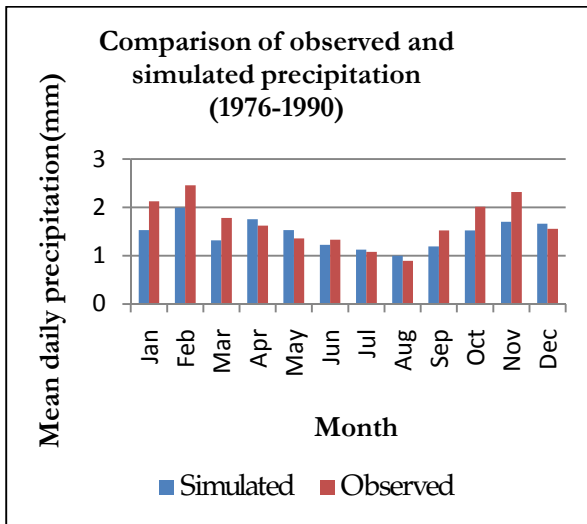


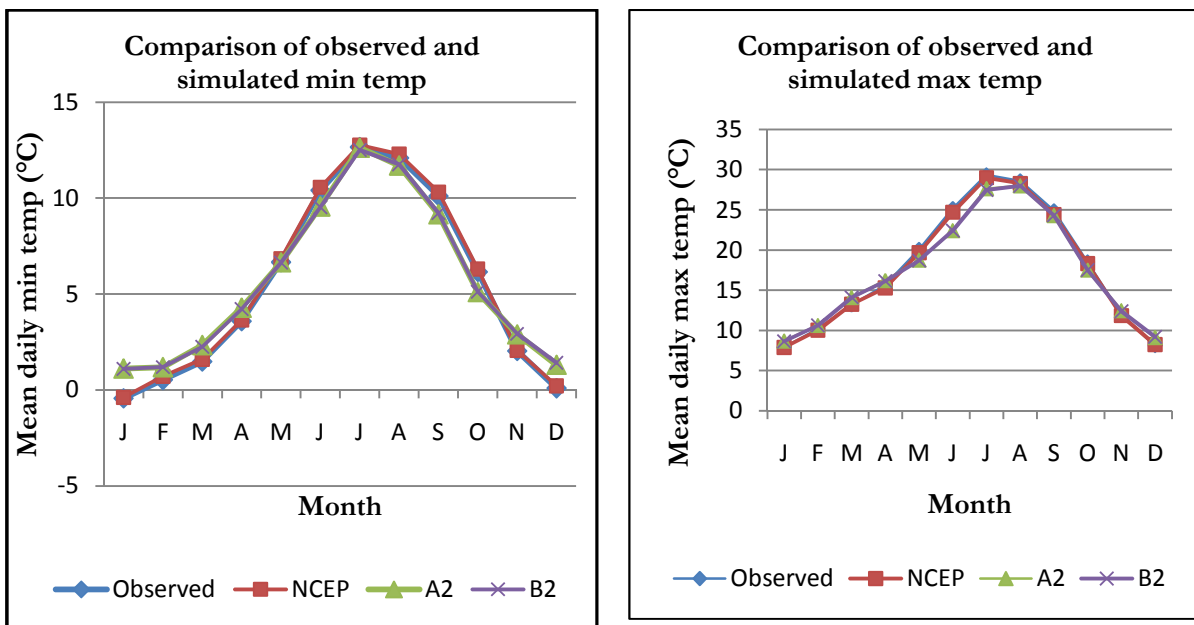
Figure 6-2: Validation results of SDSM downscaling at Trabadillo station.

Figure 6-2 shows the performance of the downscaling model for temperature and precipitation during validation. The graphs show a good agreement between the simulated and observed mean daily minimum and maximum temperature for all the months. There is also good agreement for observed and simulated mean daily precipitation for all months except January, February, March, September, October and November where the model underestimates the observed values. Values of R^2 were 0.16, 0.89 and 0.95 for precipitation, minimum temperatures and maximum temperatures respectively.

c) Downscaling present (observed) climate

The results obtained for downscaling the present climate using NCEP and HadCM3 predictors are shown below.

Figure 6-3 below shows a satisfactory agreement between the observed and simulated temperature and precipitation. A2 and B2 however overestimate January precipitation.



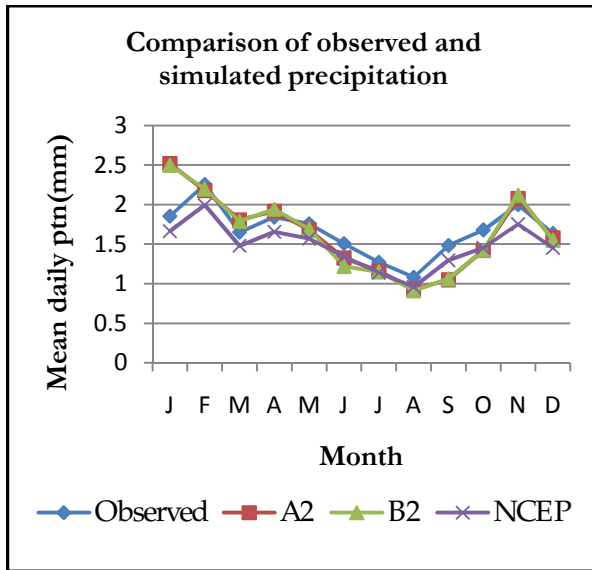
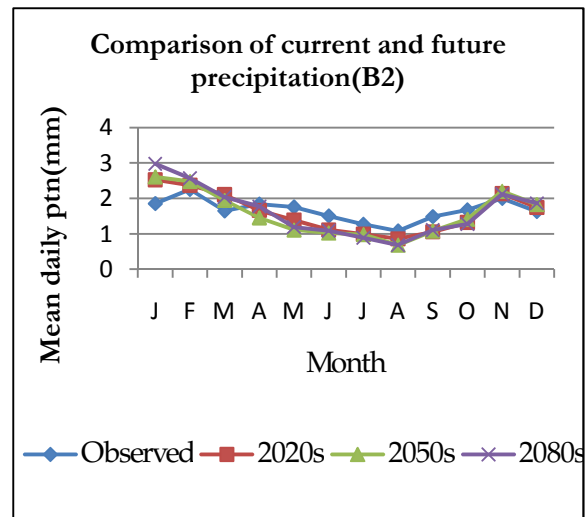
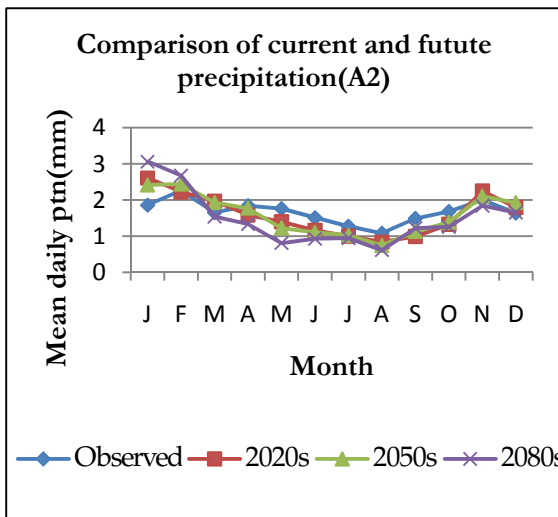
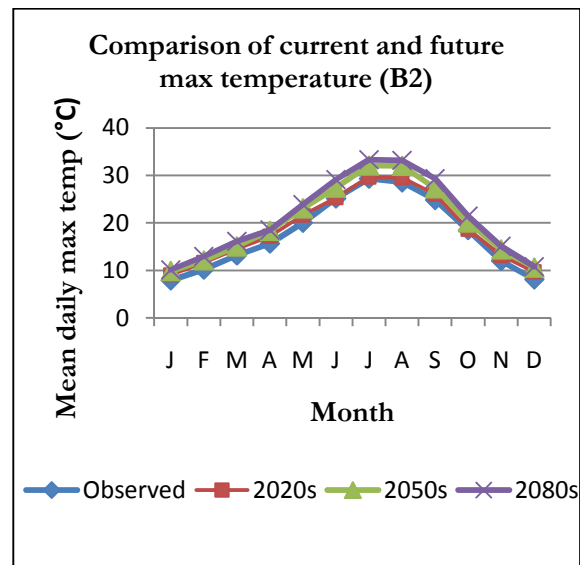
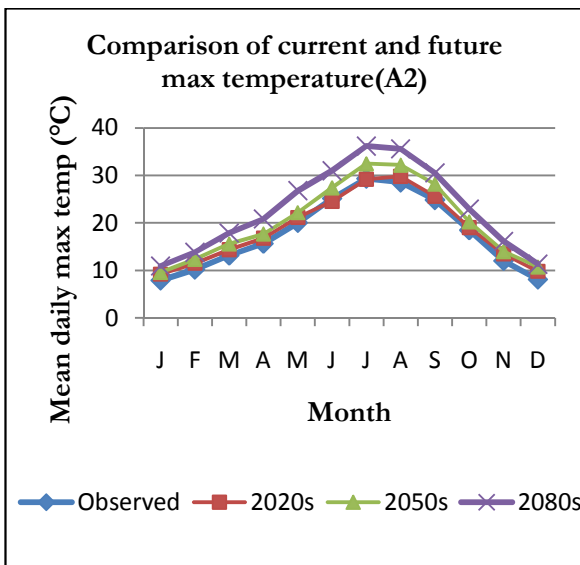
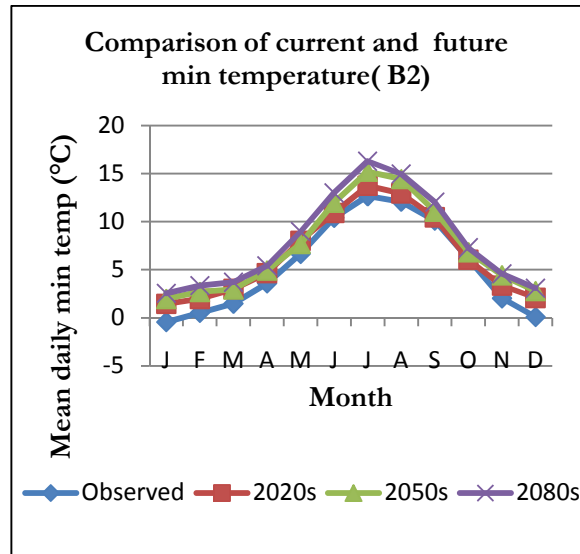
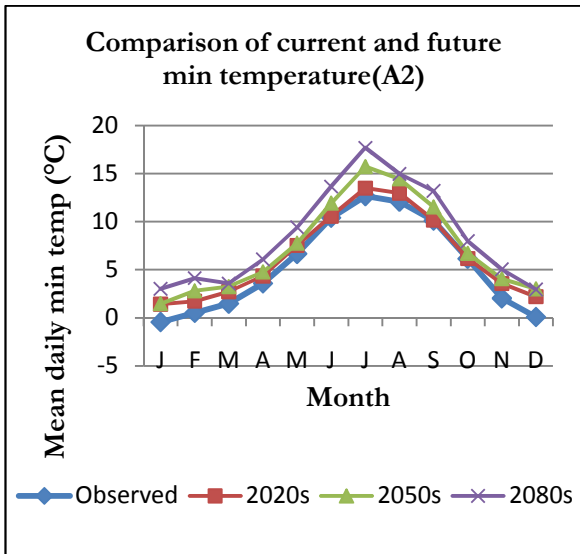


Figure 6-3: Observed 1961-90 mean daily precipitation, min and max temperature and simulated data.

d) Downscaling future climate

The results of downscaling the future climate using HadCM3 are shown in the figures below.





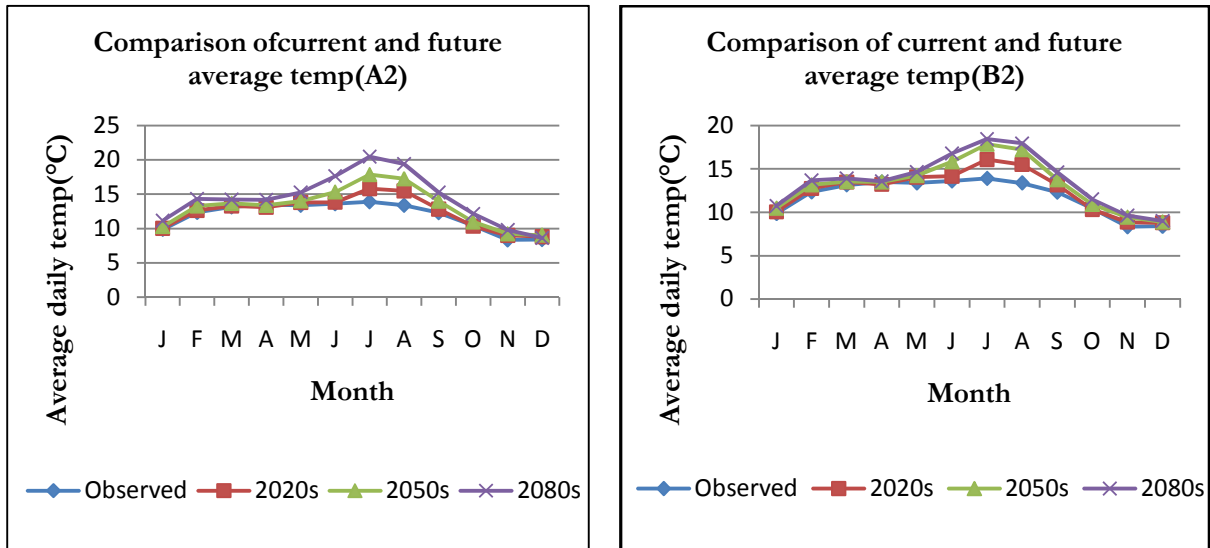


Figure 6-4: Comparison of current (1961-1990) mean daily precipitation, average temperature, minimum and maximum temperatures with future HadCM3 simulated data for the A2 and B2 scenarios

Precipitation

There is a decrease of mean daily precipitation of between 2% and 54% from April to October for both A2 and B2 scenarios, with largest decreases in late Spring (MAM) and Summer (JJA). Increases of between 1% and 65% which are largest in January, are projected from November to March. Except for the 2080s, generally decreases are greater under the B2 scenario while increases are greater under the A2 scenario except for the 2050s, when compared to the baseline period.

Annual precipitation decreases for both A2 and B2 scenarios by between 3% and 12% when compared to the baseline period. These projections are in agreement with those obtained by Castro *et al.*, (2002) where six AOGMS and a regional model were used to simulate the future climate for Spain. Their results indicate decreasing annual precipitation in the future, somewhat greater in scenario A2 than B2 and the reductions are maximum in spring and lower in summer.

Temperature

- Minimum Temperature

Mean daily minimum temperatures will generally increase by 0.007°C to 2.1°C in the 2020s, 0.5°C to 3.1°C in the 2050s and 1.1°C to 5.0°C for the 2080s for much of the year with greater increases for the A2 than B2 scenario. The increases become progressively bigger from the 2020s to the 2080s.

Greatest increases are projected in summer (JJA). There is a decrease of 0.1°C for the 2020s B2 period when compared to the baseline.

- Maximum temperature

Increases in mean daily maximum temperature of between 0.2°C to 1.7°C, 1.6°C to 3.6°C and 2.2°C to 7.0°C are forecast for the 2020s, 2050s and 2080s respectively. The A2 scenario shows higher increases

than the B2 scenario. The greatest increases are also forecast for summer (JJA). There are decreases of 0.2°C and 0.4°C in June and July respectively for the A2 2020s period when compared to the baseline.

- Average temperature

Temperature increases of up to 1.9°C, 3.1°C and 5.9°C are forecast for the 2020s, 2050s and 2080s respectively, with A2 temperatures being higher than B2 temperatures. However there is also a decrease of 0.2°C forecast in A2 2020s period for June. More warming is forecast for summer than winter.

6.4. Recharge Modeling with pyEARTH

The recharge model used daily rain and PET data as model input variables, in addition to the hydraulic head series and soil moisture data.

Figure 6-2 shows the calibration graphs for hydraulic head, recharge, soil moisture, precipitation, precipitation excess, potential evapotranspiration and actual evapotranspiration for the period 2004 to 2008. The parameters used in the calibration are shown in Appendix 1.

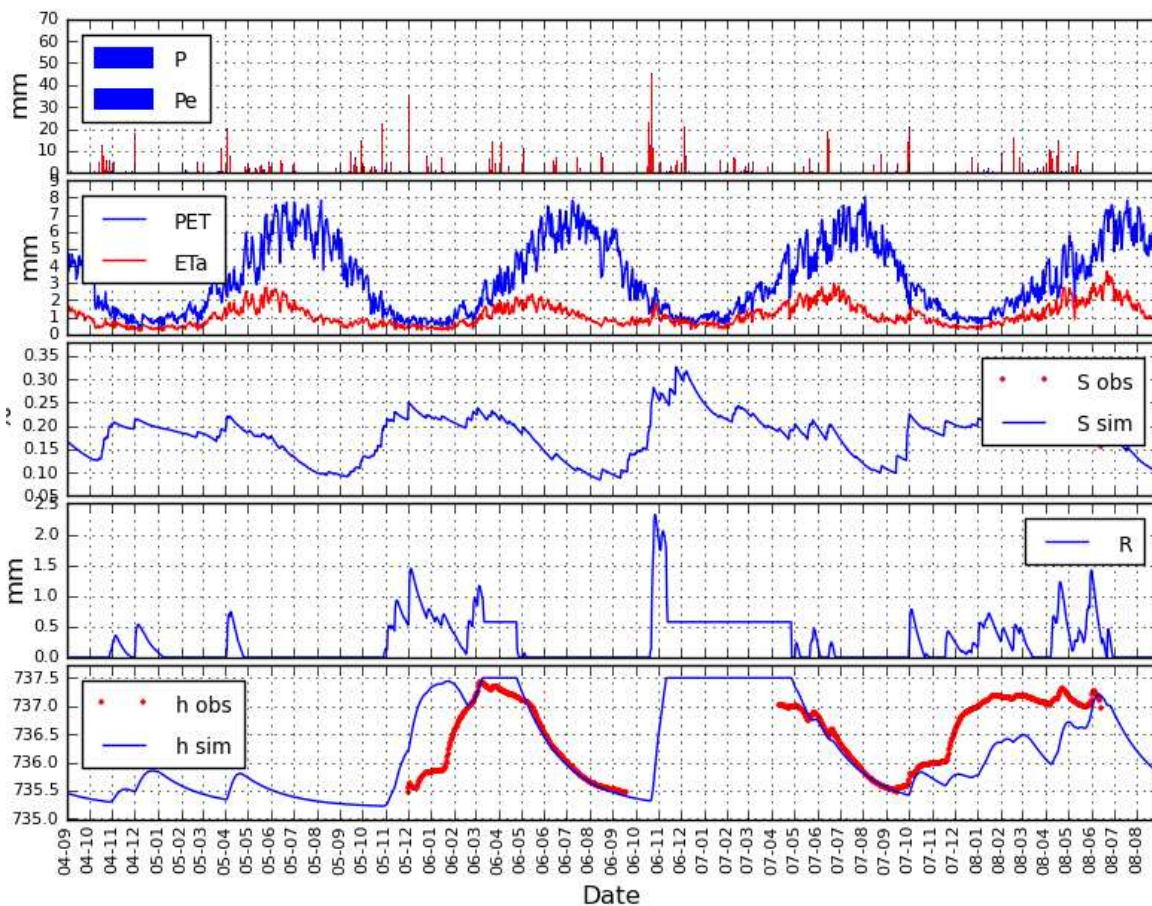


Figure 6-5: Calibration graphs for the period 2004 to 2008

Table 6-3: Results of pyEARTH 1-D Modeling

Period	Total Precipitation (mm)	Annual Precipitation (mm)	Total Recharge (mm)	Annual Recharge (mm)	Recharge (% of rainfall)
2004-2008	2269.24		370.03		16.3%
1961-1990	18212.6	607.09	2969.07	98.97	16.3%
A2(2010-2039)	17201.85	573.39	2171.38	72.38	12.6%
B2(2010-2039)	17335.83	577.86	2346.56	78.22	13.5%

These results show that annual recharge decreases by 26.87% and 20.97% for the A2 and B2 scenarios respectively for the 2020s compared to the baseline period. It should be noted that the magnitudes of recharge in the future scenarios are dependent on the values used for the parameters during calibration, with different parameters giving different recharge values. Annual precipitation decreases by 5.7% and 4.9% for the A2 and B2 scenarios respectively during the same period. The decrease in recharge in the future can be explained by decrease of rainfall during the same period.

6.5. Groundwater Modeling

Calibration and parameter settings

The optimum calibration was achieved with settings of specific yield of 0.05 to 0.1 for the first layer and 0.25 for the second layer. Specific storage was set at 0.0001 in the first layer and ranged from 0.001 to 0.0000001 in the second layer. Horizontal hydraulic conductivity (K_h) for the second layer varied from 0.3 to 24.8 while for the first layer it was 0.15 close to the Sardon river and 1 elsewhere. These settings are indicated in Figure 6-6 below. The first diagram shows hydraulic conductivity K value settings in the second layer while the second figure shows hydraulic conductivity settings in the first layer. The third figure shows value settings for specific storage Ss while the last figure shows settings for specific yield, Sy. Figure 6-7 shows the calibration performance for the 5 piezometers.

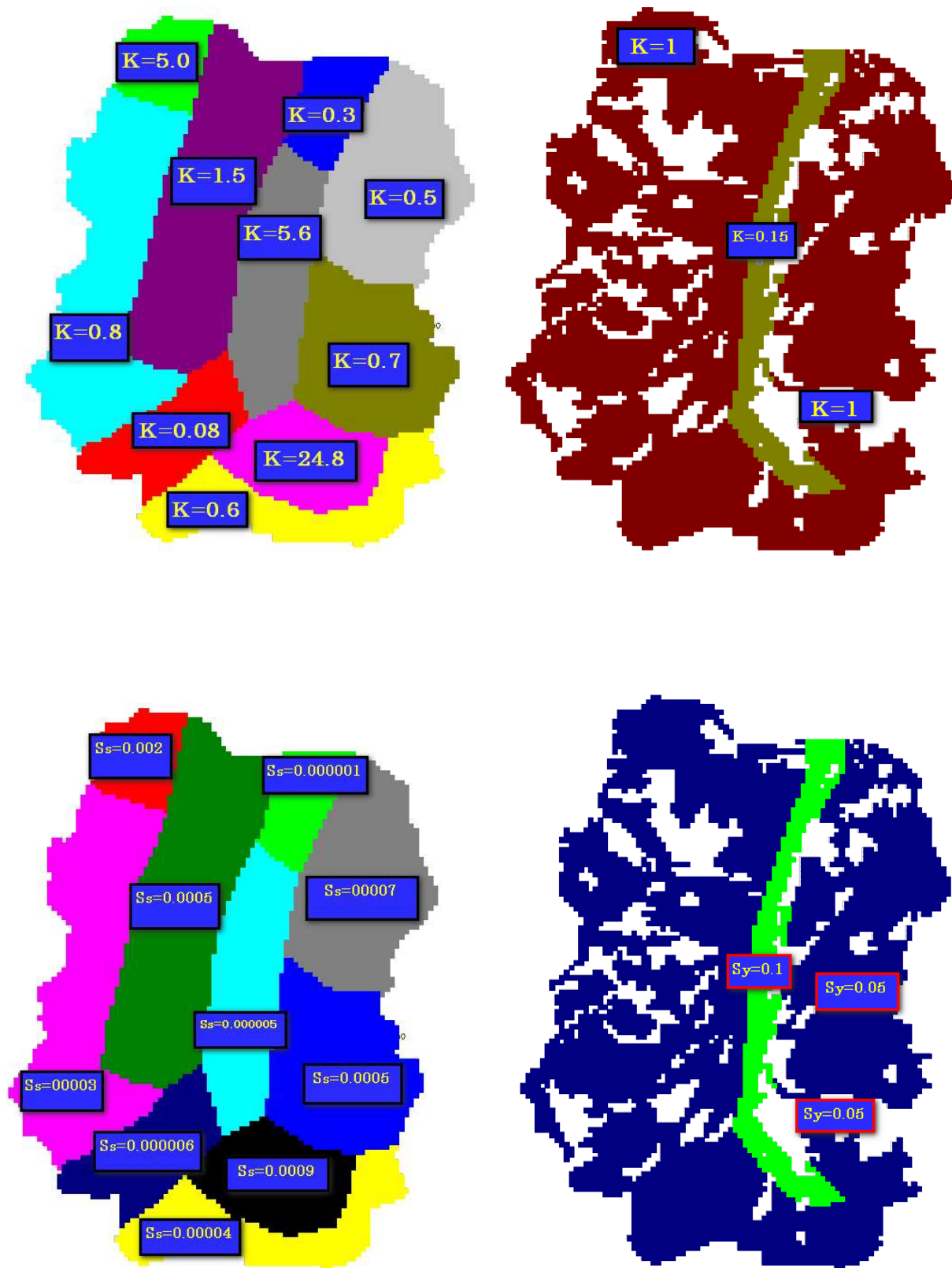
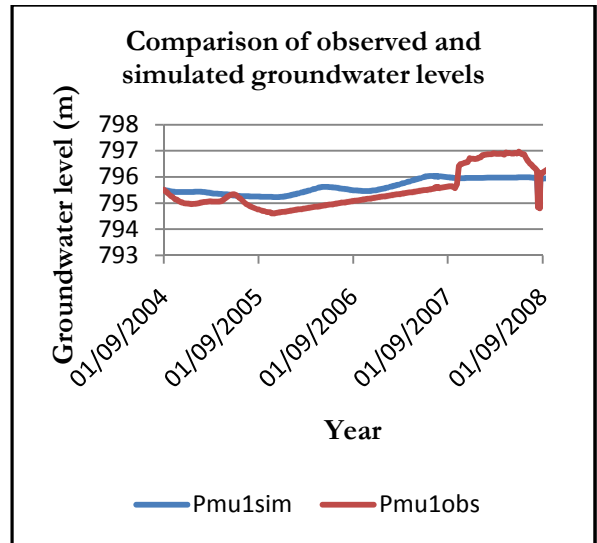
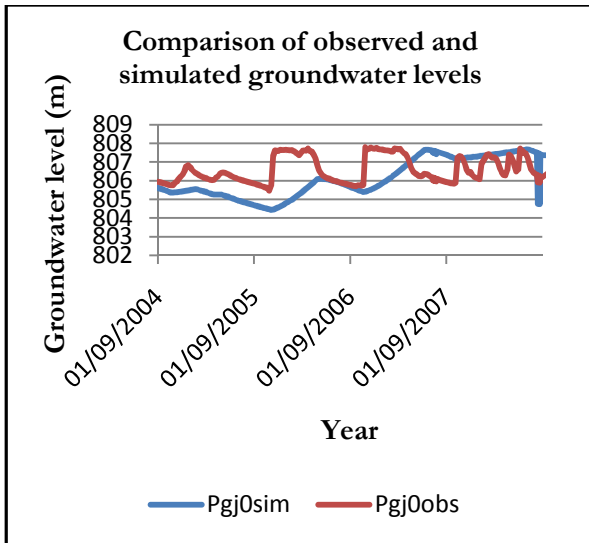
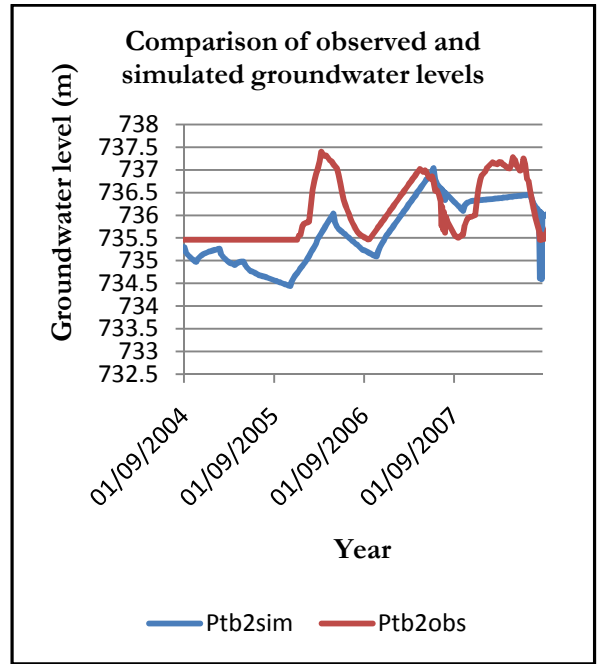
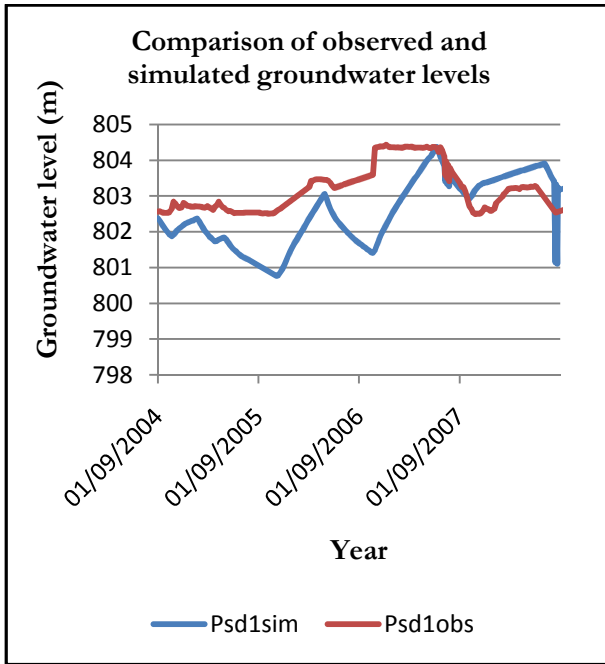


Figure 6-6: Calibration values of K, Sy and Ss for the two model layers



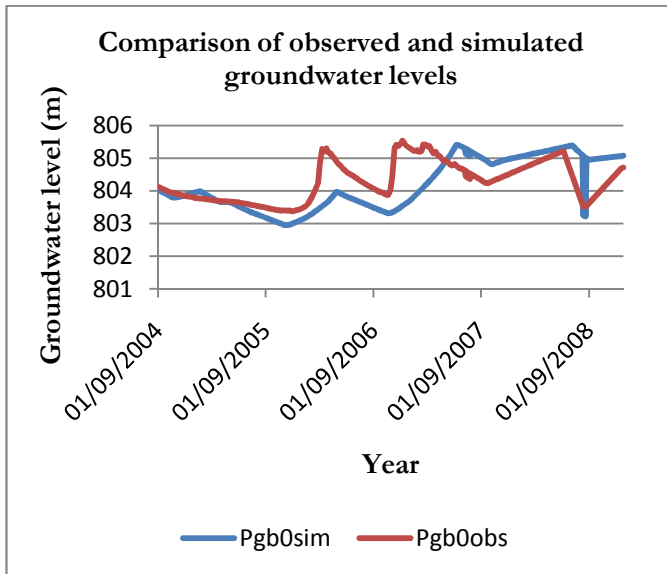


Figure 6-7: MODFLOW calibration head data in piezometers: Pgb0, Pgj0, Pmu1, Psc1 and Ptb2 (see Fig4-3) for the calibration period 2004-2008

Time series of the prediction of groundwater levels

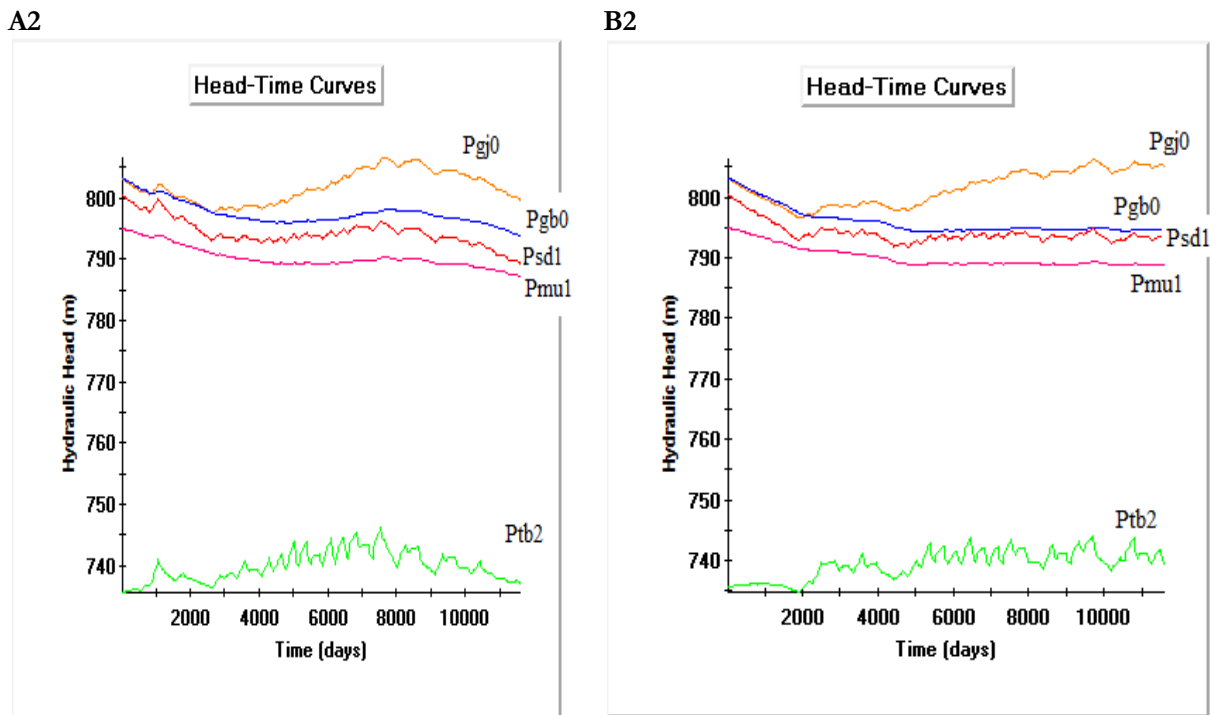


Figure 6-8: Prediction of groundwater levels of the 5 piezometers for the A2 and B2 scenarios (2010-2039)

Table 6-4: Change in groundwater levels for the 5 piezometers for the 2020s

Piezometer	Initial gw levels(m)	Final gw levels(m)(A2)	Final gw levels(m)(B2)	Change in gw levels(m)(A2)	Change in gw levels(m)(B2)
Pgs0	800.9243	799.4774	804.7903	-1.4469	3.866
Ptb2	735.9238	736.924	739.134	1.0002	3.2102
Pgb0	801.3917	793.6788	794.4551	-7.7129	-6.9366
Pmul	794.0138	787.0078	788.6492	-7.006	-5.3646
Psd1	798.0032	789.0125	792.6947	-8.9907	-5.3085

Figure 6-9 shows the variation of groundwater levels for the 5 piezometers from the beginning of 2010 to the end of 2039. In the A2 scenario groundwater levels in the four piezometers, Pgb0, Pgs0, Psd1 and Pmul decrease ranging from 1.4m to approximately 9.0 m whereas piezometer Ptb2's groundwater level increases by 1.0 m. In the B2 scenario groundwater levels in Ptb2 and Pgs0 increase by 3.2 m and 3.9 m respectively while the levels in the other three piezometers decrease by values ranging from 5.3 m to 6.9 m. Decreases in both scenarios are larger under the A2 scenario than under the B2 scenario. This can be explained by higher ETg values under the A2 than B2 scenario and also because amounts lost as drain are greater under the A2 than B2 scenario. The rises in groundwater levels for the two piezometers can be attributed to some calibration or other model errors. (Scibek & Allen, 2006b) point out that the ability of a groundwater flow model to predict changes to groundwater levels as forced by climate change depends on the locations and types of model boundary conditions, the success of model calibration and model scale.

Water Balance

Table 6-5 below shows the total water balance components for the A2 and B2 scenarios for 2010-2039 with the fluxes being given in m³. Figure 6-10 shows variation of the three water balance components from 2010 to 2039 for the two scenarios. When the catchment is taken as whole groundwater storage decreases by 24.2% under the A2 scenario and by 10.9% under the B2 scenario. Although there are year to year variations in drain and recharge, cumulative totals at the end of the simulation period indicate that water lost as drain is higher under the A2 than B2 scenario. Consequently this increase in drain coupled with a decrease in precipitation results in smaller recharge for the A2 scenario. This connection between different fluxes is further amplified by (Croley & Luukkonen, 2003) who point out that, “because groundwater resources are naturally replenished by infiltration of precipitation and subsequent percolation of water through geologic materials, a decline in precipitation or an increase in evapotranspiration would result in a decline in recharge, possibly resulting in a decline in groundwater levels.”

Table 6-5: Water balance components under the A2 and B2 scenarios for 2010-2039

	A2(IN)	A2(OUT)	B2(IN)	B2(OUT)
Recharge	2151063.9		2255798.0	
Storage	821443.5	622947.6	720835.3	641983.6
Drain		-2382240.7		-2377055.0

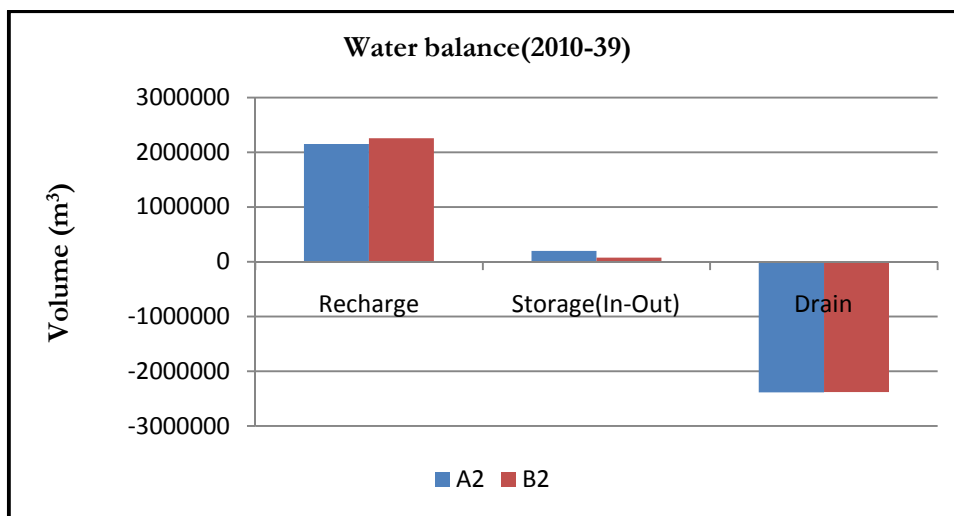
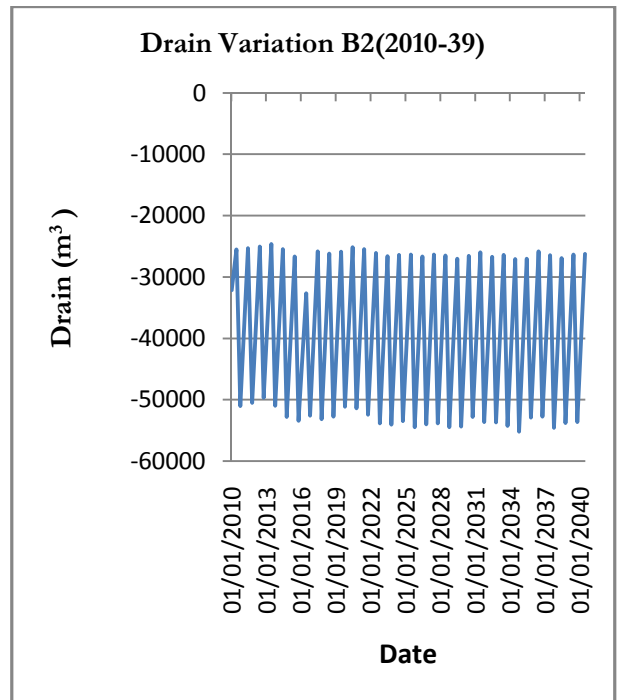
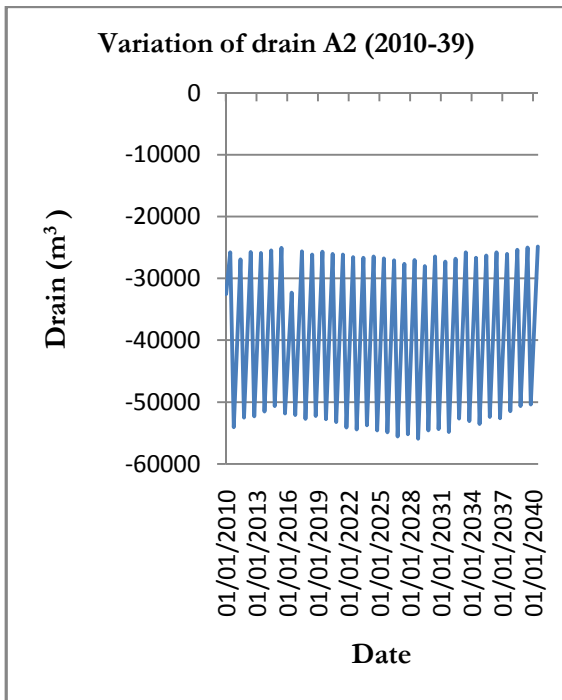
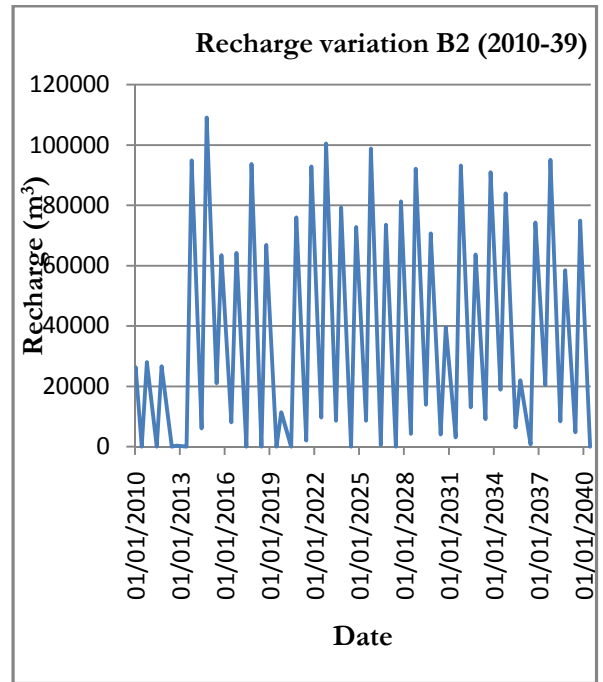
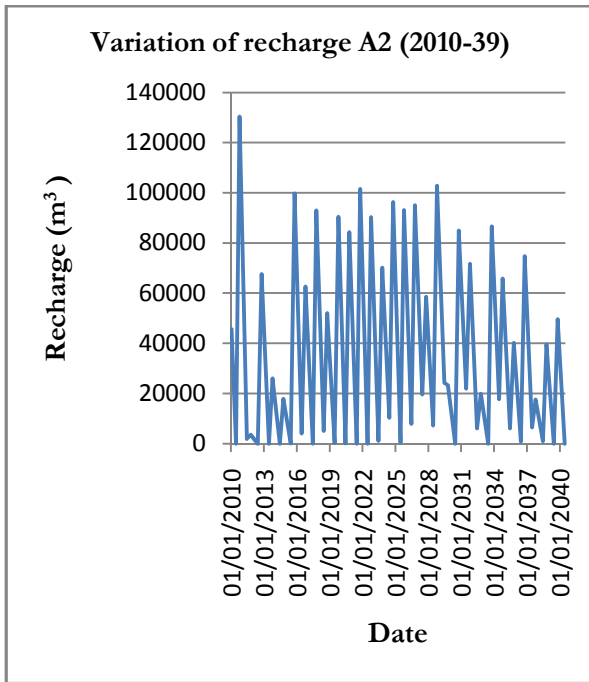


Figure 6-9: Graphical Representation of water balance components for the A2 and B2 scenarios for 2010-2039



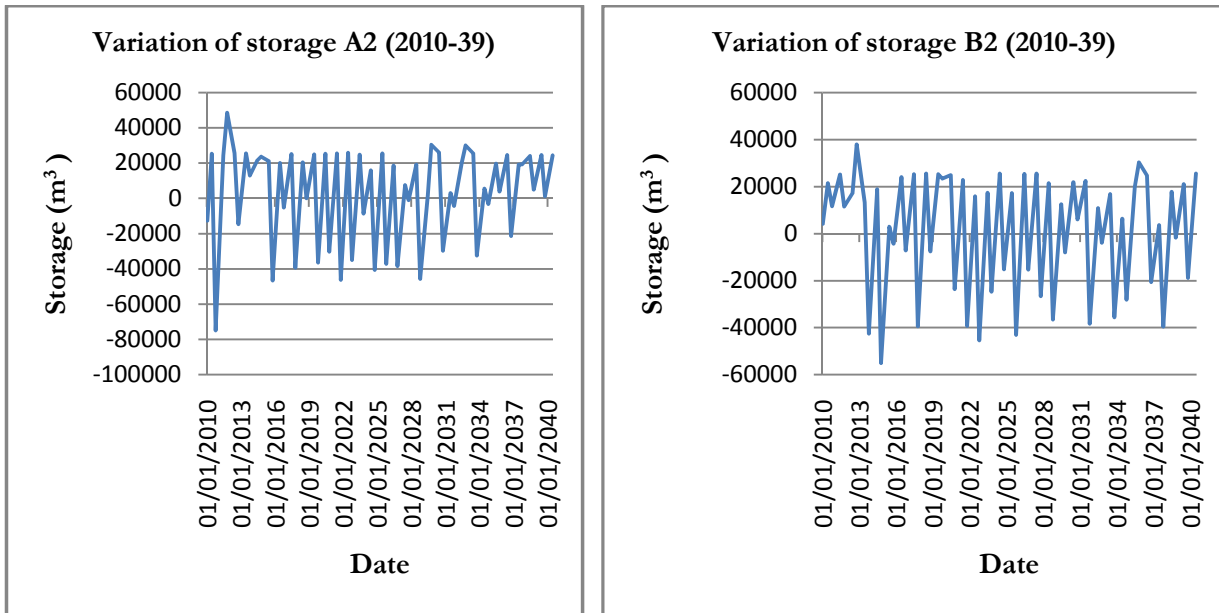


Figure 6-10: Variation of recharge, drain and storage for the A2 and B2 scenario for 2010-39

7. CONCLUSION AND RECOMMENDATIONS

7.1. Conclusion

Results of the study show that the Sardon catchment is sensitive to climate change. Maximum and average temperatures have been on an upward trend since 1956 averaging an increase of 0.38°C and 0.21°C respectively relative to the baseline period. Precipitation and minimum temperatures have not shown a clear trend although interannual variability has been noted. In the future annual precipitation is expected to decrease by between 3 % and 12% by 2099 under the A2 scenario. For the B2 scenario precipitation is expected to decrease by 4.9%, 7.2% and 3.4% respectively for the 2020s, 2050s and 2080s when compared to the baseline period. An increase in temperature is projected throughout the century with higher temperatures expected under the A2 than B2 scenario. More warming is forecasted for summer than winter. Mean daily minimum temperatures, maximum temperatures and average temperatures are forecasted to increase by up to 5.0°C, 7.0° C and 5.9°C by the end of the century.

The Statistical Downscaling Model (SDSM) was shown to be able to successfully downscale GCM output particularly minimum and maximum temperature. However in this case study it tends to miss extreme rainfall events such as high rainfall occurrences leading to a forecast of rainfall of almost uniform low intensity throughout the forecast period. This is also noted by Wilby *et al.* (2004) who point out that statistical downscaling methods are usually not very effective for simulation of extreme events of precipitation.

Simulation of recharge by the hydrological model pyEARTH 1-D indicates that recharge will decrease from the current (1961-1990) value of 16.3% of precipitation to 12.6% and 13.5% of precipitation for the 2020s A2 and B2 periods respectively. These decreases in recharge can be attributed to the decreasing precipitation within the same time period.

The groundwater model, MODFLOW was also able to simulate future changes in groundwater levels thereby allowing the quantification of climatic impacts on groundwater resources to be made. In the 2020s groundwater storage is expected to decrease by 24.2% under the A2 scenario and by 10.9% under the B2 scenario. Loss of water through drain is higher under the A2 than B2 scenario. This together with decreasing precipitation results in less recharge to the aquifer for the A2 scenario when compared to the B2 scenario. When compared to the baseline period, recharge decreases for the 2020s under both scenarios.

7.2. Recommendations

The quantification of hydrological impacts of climate change has many uncertainties. The results of this study should therefore be viewed with caution and be considered as possible not conclusive outcome as they are based on the analysis of data for one station and not all the stations in the catchment. To improve on the quality of data there is need to improve the observation network since climate data generation methods can never fully reproduce observed data.

Other methods of generating climate data such as using the LARS-WG, WXGEN and ClimGen need to be considered although these have limitations in that they require observed data of at least a specific duration to be able to generate usable data.

There is need to explore further other methods of downscaling precipitation. Even different statistical downscaling methods have yielded results showing significantly different hydrological impacts for the same catchment (Dibike & Coulibaly, 2005). Multiple linear regression techniques such as those used in SDSM are based on the assumption that the predictor-predictand relationships developed for the historical period are time-invariant. Latest research however shows that this assumption is not always true (Wilby & Wigley, 1997). In addition downscaling methodology has also been found to be area specific. It is therefore good practice to try different downscaling methods in order to find the most suitable for the area of interest.

In this study uniform recharge was applied to the catchment and the groundwater flow model run in transient to simulate impacts on water resources. In reality however recharge varies both temporally and spatially (Lubczynski & Gurwin, 2005). Further studies to see how groundwater will respond to spatially varying recharge would be useful.

The HadCM3 model was used to predict future climate scenarios. However research has shown that future projections of climate are dependent on the GCM used. It is therefore ideal to use an ensemble of GCMs that will indicate an average future scenario.

Although the pyEARTH 1-D can be used successfully in this catchment it has its own weaknesses such as the fact that it ignores lateral flow resulting in erroneous results. The use of other methods of recharge estimation such as lysimeters, well hydrographs and chloride mass balance will enable comparison of results.

Only two scenarios A2 and B2 were considered in this study. However these are just two cases of possible greenhouse emission paths. It would be informative to compare results obtained under these scenarios with results under other scenarios such as A1B and B1.

LIST OF REFERENCES

- Alley, W. M. (2001). Ground Water and Climate. *Ground Water*, 39(2), 161-161.
- Anderson, M. P., & Woessner, W. W. (1992). *Applied Groundwater Modeling: Simulation of Flow and Advective Transport*: Academic Press, Inc.
- Attanayake. (1999). Analysis of fractures in a granitic terrain and their tectonic and hydrogeological implications: a study from Sardon catchment area, Salamanca province, Spain. Unpublished MSc Thesis. ITC.
- Bear, J., Beljin, M. S., & Poss, R. R. (1992). Fundamentals of Ground-Water Modeling. *Ground Water Issue*.
- Berhe, E. T. (2010). Improving groundwater model reliability by coupling unsaturated and saturated models: a case study of Sardon catchment, Spain. Unpublished MSc Thesis. ITC.
- Castro, M. d., Martín-Vide, J., & Alonso, S. (2002). *The climate of Spain: past, present and scenarios for the 21st century*.
- Chen, Y. D., Chen, Y., Xu, X. Y., & Shao, Q. (2006). Downscaling of daily precipitation with a stochastic weather generator for the subtropical region in South China. *Hydrology and Earth System Sciences Discussion*, 3, 1-39.
- Cornejo, S. P. U. (2000). Groundwater recharge modelling in hard rocks area : Sardon case study, Spain. Unpublished MSc Thesis. ITC.
- Croley, T. E., & Luukkonen, C. L. (2003). Potential effects of climate change on groundwater in Lansing, Michigan. *JAWRA Journal of the American Water Resources Association*, 39(1), 149-163.
- Dibike, Y. B., & Coulibaly, P. (2005). Hydrologic impact of climate change in the Saguenay watershed: comparison of downscaling methods and hydrologic models. *Journal of Hydrology*, 307(1-4), 145-163.
- Dingman, S. L. (2002). *Physical Hydrology* (Second Edition ed.): Prentice Hall.
- Douglas, E. M., Vogel, R. M., & Kroll, C. N. (2000). Trends in floods and low flows in the United States: impact of spatial correlation. [doi: DOI: 10.1016/S0022-1694(00)00336-X]. *Journal of Hydrology*, 240(1-2), 90-105.
- Doyle, J. D. (1997). The Influence of Mesoscale Orography on a Coastal Jet and Rainband. *Monthly Weather Review*, 125(7), 1465-1488.
- Duah, A. A. (1999). *Groundwater recharge modeling in hard rocks using remote sensing and GIS applications(A case study in the lower Rio Tormes basin, Salamanca Province, Spain)*. Unpublished MSc, University of Twente.
- Fowler, H. J., Blenkinsop, S., & Tebaldib, C. (2007). Linking climate change modelling to impacts studies: recent advances in downscaling techniques for hydrological modelling. *International Journal of Climatology*, 27, 1547-1578.
- Frances, A. P. (2008). Spatio-temporal groundwater recharge assessment : a data-integration and modelling approach
Unpublished MSc Thesis. ITC.
- Freeze, A. R., & Cherry, J. A. (1979). *Groundwater*: Prentice Hall.
- Gellens, D. (1991). Impact of a CO₂-induced climatic change on river flow variability in three rivers in Belgium. *Earth Surface Processes and Landforms*, 16(7), 619-625.
- Gieske, A. (1992). *Dynamics of groundwater recharge: a case study in semi arid Botswana*. Unpublished PhD Thesis, Vrije Universiteit, Amsterdam.
- Goderniaux, P., Brouyere, S., Fowler, H. J., Blenkinsop, S., Therrien, R., Orban, P., et al. (2009). Large scale surface-subsurface hydrological model to assess climate change impacts on groundwater reserves. *Journal of Hydrology*, 373(1), 122-138.
- Healy, R. W., & Cook, P. G. (2002). Using groundwater levels to estimate recharge. *Hydrogeology Journal*, 1-19.
- Hillel, D. (1982). *Introduction to soil physics*: Academic Press
- Houghton, J. T., Ding, Y., Griggs, D. J., Noguer, M., Linden, P. J. v. d., Dai, X., et al. (2001). Climate Change 2001: The Scientific Basis. Contribution of Working Group I to the Third Assessment Report of the Intergovernmental Panel on Climate Change (pp. 881pp.): Cambridge University Press, Cambridge, United Kingdom and New York, NY, USA.
- Huntington, T. G. (2006). Evidence for intensification of the global water cycle: Review and synthesis. [doi: DOI: 10.1016/j.jhydrol.2005.07.003]. *Journal of Hydrology*, 319(1-4), 83-95.

- Jyrkama, M. I., & Sykes, J. F. (2007). The impact of climate change on spatially varying groundwater recharge in the grand river watershed (Ontario). [doi: DOI: 10.1016/j.jhydrol.2007.02.036]. *Journal of Hydrology*, 338(3-4), 237-250.
- Kahya, E., & Kalayci, S. (2004). Trend analysis of streamflow in Turkey. [doi: DOI: 10.1016/j.jhydrol.2003.11.006]. *Journal of Hydrology*, 289(1-4), 128-144.
- Kemper, K. (2004). Groundwater—from development to management. [10.1007/s10040-003-0305-1]. *Hydrogeology Journal*, 12(1), 3-5.
- Kirchner, J. (2003). *Changing rainfall – changing recharge?* : UNESCO IHP.
- Kundzewicz, Z. W., & Robson, A. (2000). *Detecting Trend and Other Changes in Hydrological Data*. World Climate Program – Water, WMO/ UNESCO, WCDMP-45, WMO/ TD 1013, Geneva. Unpublished manuscript.
- Lee, J. v. d., & Gehrels, J. C. (1990). *Modeling Aquifer Recharge : Introduction to the lumped parameter model Earth*. Free University of Amsterdam.
- Lerner, D. N., Issar, A. S., & Simmers, I. (1990). Groundwater recharge: A guide to understanding and estimating natural recharge. . *International Contributions to Hydrogeology*, 8.
- Lubczynski, M. W., & Gurwin, J. (2005). Integration of various data sources for transient groundwater modeling with spatio - temporally variable fluxes : Sardon study case, Spain. *Journal of hydrology*, 306((1-4)), 71-96.
- McDonald, M. G., & Harbaugh, A. W. (1988). A Modular Three-Dimensional Finite-Difference Ground-Water Flow Model: U. S. Geological Survey.
- Mearns, L. O., Giorgi, F., McDaniel, L., & Shields, C. (2003). Climate Scenarios for the Southeastern U.S. Based on GCM and Regional Model Simulations. *Clim. Change*, 60, 7-35.
- Nakicenovic, N., Alcamo, J., Davis, G., Vries, B. d., Fenhann, J., S.Gaffin, et al. (2000). *IPCC Special Report on Emissions Scenarios*: Cambridge University Press, Cambridge, United Kingdom
- Nguyen, V.-T.-V., Nguyen, T.-D., & Gachon, P. (2004). *On the linkage of large-scale climate variability with local characteristics of daily precipitation and temperature extremes: an evaluation of statistical downscaling methods*. Unpublished manuscript.
- O'Hare, G., Sweeney, J., & R.Wilby. (2005). Weather, climate and climate change: Human perspectives (pp. 403pp): Pearson Education, Harlow.
- Obakeng, O. (2007). Soil moisture dynamics and evapotranspiration at the fringe of the Botswana Kalahari, with emphasis on deep rooting vegetation. Unpublished PhD Thesis. Vrije Universiteit.
- Ontiveros, E. R. (2009). Tree transportation : a spatio - temporal approach in water limited environments, Sardon study case. Unpublished MSc Thesis. ITC.
- Rajapakse, R. G. (2009). Numerical groundwater flow and solute transport modelling : a case study of Sardon catchment in Spain. Unpublished MSc Thesis. ITC.
- Scibek, J., & Allen, D. M. (2006a). Comparing modelled responses of two high-permeability, unconfined aquifers to predicted climate change. [doi: DOI: 10.1016/j.gloplacha.2005.10.002]. *Global and Planetary Change*, 50(1-2), 50-62.
- Scibek, J., & Allen, D. M. (2006b). Modeled impacts of predicted climate change on recharge and groundwater levels. *Water Resources Research*, 42(11), W11405.
- Shakya, D. R. (2001). Spatial and temporal groundwater modeling integrated with remote sensing and GIS : hard rock experimental catchment, Sardon.Spain. Unpublished MSc Thesis. ITC.
- Sophocleous, M. (2004). Climate Change: Why Should Water Professionals Care? *Ground Water*, 42(5), 637-637.
- Sullivan, C. (2001). The Potential for Calculating a Meaningful Water Poverty Index. *Water International*, 26(4), 471 - 480.
- Tesfai. (2000). Subsurface characterization of granite basement from structural and resistivity data: a case study from sardon catchment area, Salamanca, Spain. . Unpublished MSc Thesis. ITC.
- Tharme, R. É. (2003). A global perspective on environmental flow assessment: emerging trends in the development and application of environmental flow methodologies for rivers. *River research and applications*, 19, 397-441.
- Thornthwaite, C. W. (1948). An approach towards a rational classification of climate *Geogr. Rev.* (38), 55–94.
- Toews, M. (2003). Modelling climate change impacts on groundwater recharge in a semi arid region, southern Okanagan, British Columbia. Unpublished MSc Thesis. University of Calgary.
- Trajković, S., & Gocić, M. (2010). Comparison of some empirical equations for estimating daily reference evapotranspiration. *Architecture and Civil Engineering*, 8.

- Villazón, M. F., & Willems, P. (2010). Filling gaps and Daily Disaccumulation of Precipitation Data for Rainfall-runoff model.
- Wilby, R. L., & Wigley, T. M. L. (1997). Downscaling general circulation model output: a review of methods and limitations. *Progress in Physical Geography*, 21, 530-548.
- Xu, C.-y. (1999). Climate Change and Hydrologic Models: A Review of Existing Gaps and Recent Research Developments. [10.1023/A:1008190900459]. *Water Resources Management*, 13(5), 369-382.

8. APPENDICES

Appendix 8-1: pyEARTH calibration parameters for the period 2004 to 2008

SOMOS	
MAXIL (mm)	0.5
Wm (%)	0.38
Wfc (%)	0.195
Wr (%)	0.17
D (mm)	1000
Ks (mm/day)	5
SUSTm (mm)	0
LINRES	
n	1
f	0.5
SATFLOW	
RC (day)	60
STO	0.015
hi (m)	0.26
h0 (m)	735.2
Elevation (m)	737.2

Appendix 8-2: Stress periods and recharge values for A2 and B2 scenarios for 2010-2039

Stress period	Start	End	Days	Time Steps	Recharge_A2	Recharge_A2
1	15/06/2008	20/09/2008	97	3	2.42487E-05	2.42487E-05
2	21/09/2008	27/05/2009	247	8	5.57E-05	5.57E-05
3	28/05/2009	31/12/2009	217	7	0	0
4	01/01/2010	30/05/2010	150	5	0.000279956	0.000161691
5	01/06/2010	30/09/2010	120	4	0	0
6	01/10/2010	30/05/2011	240	8	0.000506574	0.000110144
7	01/06/2011	30/09/2011	120	4	0.000014375	0
8	01/10/2011	30/05/2012	240	8	1.37763E-05	0.000107614
9	01/06/2012	30/09/2012	120	4	0	0
10	01/10/2012	30/05/2013	240	8	0.000267526	1.17975E-06
11	01/06/2013	30/09/2013	120	4	0	0
12	01/10/2013	30/05/2014	240	8	0.000104112	0.000410954
13	01/06/2014	30/09/2014	120	4	0	5.27083E-05
14	01/10/2014	30/05/2015	240	8	7.33088E-05	0.000474081
15	01/06/2015	30/09/2015	120	4	1.01169E-06	0.000182083
16	01/10/2015	30/05/2016	240	8	0.000418629	0.000275437
17	01/06/2016	30/09/2016	120	4	3.35417E-05	0
18	01/10/2016	30/05/2017	240	8	0.000263333	0.000279262
19	01/06/2017	30/09/2017	120	4	0	0
20	01/10/2017	30/05/2018	240	8	0.000393804	0.00040914
21	01/06/2018	30/09/2018	120	4	4.3125E-05	0
22	01/10/2018	30/05/2019	240	8	0.00022062	0.00029241
23	01/06/2019	30/09/2019	120	4	2.36948E-06	0
24	01/10/2019	30/05/2020	240	8	0.000385201	4.98181E-05
25	01/06/2020	30/09/2020	120	4	4.80057E-07	0
26	01/10/2020	30/05/2021	240	8	0.000359072	0.000338317
27	01/06/2021	30/09/2021	120	4	0	1.83882E-05
28	01/10/2021	30/05/2022	240	8	0.00043281	0.0004159
29	01/06/2022	30/09/2022	120	4	0	8.625E-05
30	01/10/2022	30/05/2023	240	8	0.000384981	0.000450144
31	01/06/2023	30/09/2023	120	4	9.60794E-06	7.66667E-05
32	01/10/2023	30/05/2024	240	8	0.000299387	0.000355429
33	01/06/2024	30/09/2024	120	4	8.76834E-05	0
34	01/10/2024	30/05/2025	240	8	0.000410695	0.000326385
35	01/06/2025	30/09/2025	120	4	4.39085E-06	7.66668E-05
36	01/10/2025	30/05/2026	240	8	0.000397156	0.000442618
37	01/06/2026	30/09/2026	120	4	6.70835E-05	4.79167E-06
38	01/10/2026	30/05/2027	240	8	0.000405492	0.000329412
39	01/06/2027	30/09/2027	120	4	0.000167709	0
40	01/10/2027	30/05/2028	240	8	0.000249437	0.000364361
41	01/06/2028	30/09/2028	120	4	6.17833E-05	3.81617E-05
42	01/10/2028	30/05/2029	240	8	0.000438363	0.000412908

43	01/06/2029	30/09/2029	120	4	0.000206042	0.000124583
44	01/10/2029	30/05/2030	240	8	9.91592E-05	0.000316758
45	01/06/2030	30/09/2030	120	4	0	3.57467E-05
46	01/10/2030	30/05/2031	240	8	0.000362393	0.000177176
47	01/06/2031	30/09/2031	120	4	0.000186875	2.74792E-05
48	01/10/2031	30/05/2032	240	8	0.000305799	0.000417659
49	01/06/2032	30/09/2032	120	4	5.21242E-05	0.00011682
50	01/10/2032	30/05/2033	240	8	8.44719E-05	0.00028551
51	01/06/2033	30/09/2033	120	4	0	8.19821E-05
52	01/10/2033	30/05/2034	240	8	0.000369608	0.000407588
53	01/06/2034	30/09/2034	120	4	0.000151039	0.000169549
54	01/10/2034	30/05/2035	240	8	0.000280647	0.00037632
55	01/06/2035	30/09/2035	120	4	5.21107E-05	5.6812E-05
56	01/10/2035	30/05/2036	120	8	0.000171526	9.85429E-05
57	01/06/2036	30/09/2036	240	4	7.25252E-06	6.2925E-06
58	01/10/2036	30/05/2037	120	8	0.000320153	0.000333248
59	01/06/2037	30/09/2037	240	4	5.51156E-05	0.000183562
60	01/10/2037	30/05/2038	120	8	7.58599E-05	0.000426993
61	01/06/2038	30/09/2038	240	4	7.88474E-06	7.55364E-05
62	01/10/2038	30/05/2039	120	8	0.00017276	0.000262351
63	01/06/2039	30/09/2039	240	4	0	4.30315E-05
64	01/10/2039	30/05/2040	120	8	0.000221834	0.000336166
65	01/06/2040	30/09/2040	240	4	0	0
Total			11631	387		

Appendix 8-3: Total water balance (15/06/ 2004 to 30/09/2040)

VOLUMETRIC BUDGET FOR ENTIRE MODEL AT END OF TIME STEP 4 IN STRESS PERIOD 65

```

-----
CUMULATIVE VOLUMES      L**3      CUMULATIVE VOLUMES      L**3
-----
A2IN:
---
STORAGE = 27921656.0000
CONSTANT HEAD = 0.0000
DRAINS = 0.0000
RECHARGE = 66442188.0000
TOTAL IN = 94363840.0000

OUT:
----
STORAGE = 19191394.0000
CONSTANT HEAD = 0.0000
DRAINS = 76849912.0000
RECHARGE = 0.0000

TOTAL OUT = 96041304.0000
IN - OUT = -1677462.0000

B2 IN:
---
STORAGE = 24912552.0
CONSTANT HEAD = 0.0000
DRAINS = 0.0000
RECHARGE = 69003752.0
TOTAL IN = 93916304.0

OUT:
----
STORAGE = 19385406.0
CONSTANT HEAD = 0.0000
DRAINS = 76675760.0
RECHARGE = 0.0000

TOTAL OUT = 96061166.0
IN - OUT = -2144862.0

```